

Phase diagram in an effective model of QCD, the Nambu–Jona-Lasinio model with a Polyakov loop

Mesonic correlations in the “confined / chirally symmetric” phase
 (“quarkyonic” phase)

Hubert Hansen <hansen@ipnl.in2p3.fr>

18 Octobre 2010

Institut de Physique Nucléaire de Lyon, CNRS/IN2P3
et université Claude Bernard de Lyon

Collaborators: G. Goessens, P. Costa,
M. Ruivo, C. Da Sousa, W. Alberico, G. Chanfray, C. Ratti, A. Molinari, M. Nardi, A. Beraudo

Part I:

The NJL and PNJL effective model of QCD

QCD possesses (almost) the $SU(3) \times SU(3)$ chiral symmetry. At low energy, the pertinent degrees of freedom are the mesons.

✿ **Wigner realization :** for each meson, a chiral partner with (almost) the same mass exists. **False experimentally**

✿ **Spontaneous chiral symmetry breaking**

At contrary to the vector mesons, the pseudoscalar octet is off-scale light :

Spontaneous chiral symmetry breaking phenomenon from $SU(3) \times SU(3) \Rightarrow$ octet of (almost) Goldstone bosons, the pseudoscalar octet.

✿ **Case of the η**

The pseudoscalar η meson is not of the Goldstone type. Classically, QCD Lagrangian possesses (almost) the $U(N_f) \times U(N_f)$ symmetry. In fact, the Adler–Jackiw–Bell $U_A(1)$ anomaly breaks this symmetry to $SU(N_f) \times SU(N_f)$ and explain the large mass of the η even if quark masses are zero.

Origin of this anomaly : interaction with instantons change chirality.

✿ **Quark confinement and asymptotic freedom:** Z_{N_c} (center of $SU(N_c)$) can also be spontaneously broken (e.g. high temperature) \implies color deconfinement.

Nambu-Jona-Lasinio effective models

Motivated by the underlying symmetry of QCD (Ginzburg-Landau theory)

★ Extended NJL Lagrangian

$$\begin{aligned}
 \mathcal{L}_{NJL} &= \mathcal{L}_0 + \mathcal{L}_4 + \mathcal{L}_6 \\
 \mathcal{L}_0 &= \bar{q}(i\gamma^\mu \partial_\mu - \hat{m})q \\
 \mathcal{L}_4 &= G_1 \left[(\bar{q}\lambda_a q)^2 + (\bar{q}i\gamma_5 \lambda_a q)^2 \right] \\
 \mathcal{L}_6 &= g_D \left(\det_{flavor} \bar{q}P_L q + \det_{flavor} \bar{q}P_R q \right)
 \end{aligned}$$

$\bar{q} = (\bar{u}, \bar{d}, \bar{s})$, $\hat{m} = diag(m_u, m_d, m_s)$, $P_{L,R} = \frac{1 \mp \gamma_5}{2}$; λ_a , $a \in [0, 8]$: Gell-Mann matrices in flavor space

Invariant under global color symmetry $SU(N_c)$

\mathcal{L}_4 has $U_L(3) \times U_R(3)$ chiral symmetry (G_1 mimicks a frozen gluon propagator)

$\mathcal{L}_6 \Rightarrow U_A(1)$ anomaly break $U_L(3) \times U_R(3)$ to $SU_L(3) \times SU_R(3)$

$\hat{m} \Rightarrow$ explicit chiral symmetry breaks $SU_L(3) \times SU_R(3)$ to $SU_f(3)$.

In the following: **Restriction to $SU_f(N_f = 2)$**

PNJL model (Polyakov – Nambu – Jona-Lasinio)

$$\begin{aligned}\mathcal{L}_{PNJL} = & \bar{q} (i\gamma_\mu D^\mu - \hat{m}_0) q \\ & + G_1 \left[(\bar{q}q)^2 + (\bar{q}i\gamma_5 \vec{\tau} q)^2 \right] \\ & - \mathcal{U}(\Phi[A], \bar{\Phi}[A]; T) + \mu \bar{q} \gamma_0 q\end{aligned}$$

where $q = (q_u, q_d)$ are the quark fields ;

$$D^\mu = \partial^\mu - i A^\mu ;$$

$$A^\mu = g_S \mathcal{A}_a^\mu(x) \frac{\lambda_a}{2} \delta_0^\mu A^0 \text{ and } A^0 = -i A_4$$

The two-flavor current quark mass matrix is $\hat{m}_0 = \text{diag}(m_u, m_d)$ and we shall work in the isospin symmetric limit with $m_u = m_d \equiv m_0$; G_1 is the coupling strength of the chirally symmetric four-fermion interaction.

$\mathcal{U}(\Phi[A], \bar{\Phi}[A]; T)$: Polyakov loop potential (mimicks a static background gauge field)

Λ [GeV]	G_1 [GeV $^{-2}$]	m_0 [MeV]	$ \langle \bar{\psi}_u \psi_u \rangle ^{1/3}$ [MeV]	f_π [MeV]	m_π [MeV]
0.651	5.04	5.5	251	92.3	139.3

$$m = 325 \text{ MeV}$$

The PNJL model (Polyakov – Nambu – Jona-Lasinio)

$$\mathcal{L}_{PNJL} = \bar{q} (i\gamma_\mu D^\mu - \hat{m}_0) q + G_1 \left[(\bar{q}q)^2 + (\bar{q}i\gamma_5 \vec{\tau} q)^2 \right] - \mathcal{U}(\Phi[A], \bar{\Phi}[A]; T) + \mu \bar{q} \gamma_0 q$$

where $q = (q_u, q_d)$ are the quark fields and $D^\mu = \partial^\mu - iA^\mu$

Λ [GeV]	G_1 [GeV $^{-2}$]	m_0 [MeV]	$ \langle \bar{\psi}_u \psi_u \rangle ^{1/3}$ [MeV]	f_π [MeV]	m_π [MeV]
0.651	5.04	5.5	251	92.3	139.3

$$m = 325 \text{ MeV}$$

* Polyakov loop in imaginary time and Polyakov gauge $A_\mu = \delta_{\mu 4} A_4$

$$L(\vec{x}) = \mathcal{P} \exp \left[i \int_0^\beta d\tau A_4(\vec{x}, \tau) \right] \Rightarrow \text{effective field } \Phi = \frac{1}{N_c} \text{Tr}_C L$$

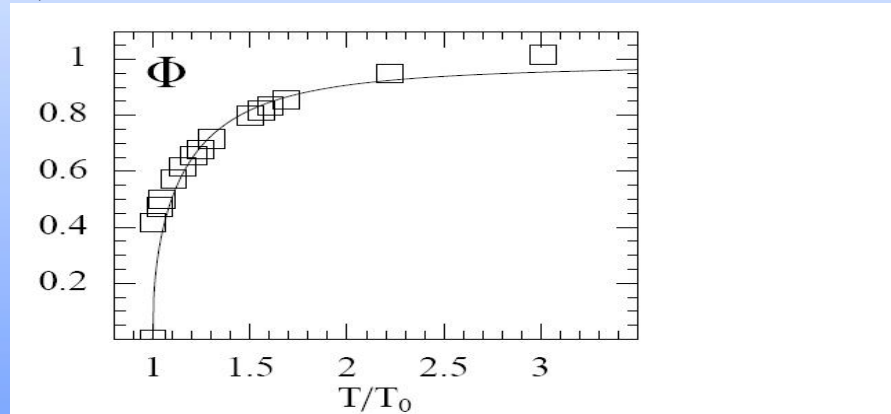
$A_4 = iA^0$: temporal component of the Euclidean gauge field (\vec{A}, A_4) , \mathcal{P} : path ordering.

* Effective potential $\mathcal{U}(\Phi, \bar{\Phi}; T)$: $T_0 = 270$ MeV

$$\frac{\mathcal{U}(\Phi, \bar{\Phi}; T)}{T^4} = -\frac{b_2(T)}{2} \bar{\Phi} \Phi - \frac{b_3}{6} (\Phi^3 + \bar{\Phi}^3) + \frac{b_4}{4} (\bar{\Phi} \Phi)^2 \text{ and}$$

$$b_2(T) = a_0 + a_1 \left(\frac{T_0}{T} \right) + a_2 \left(\frac{T_0}{T} \right)^2 + a_3 \left(\frac{T_0}{T} \right)^3 .$$

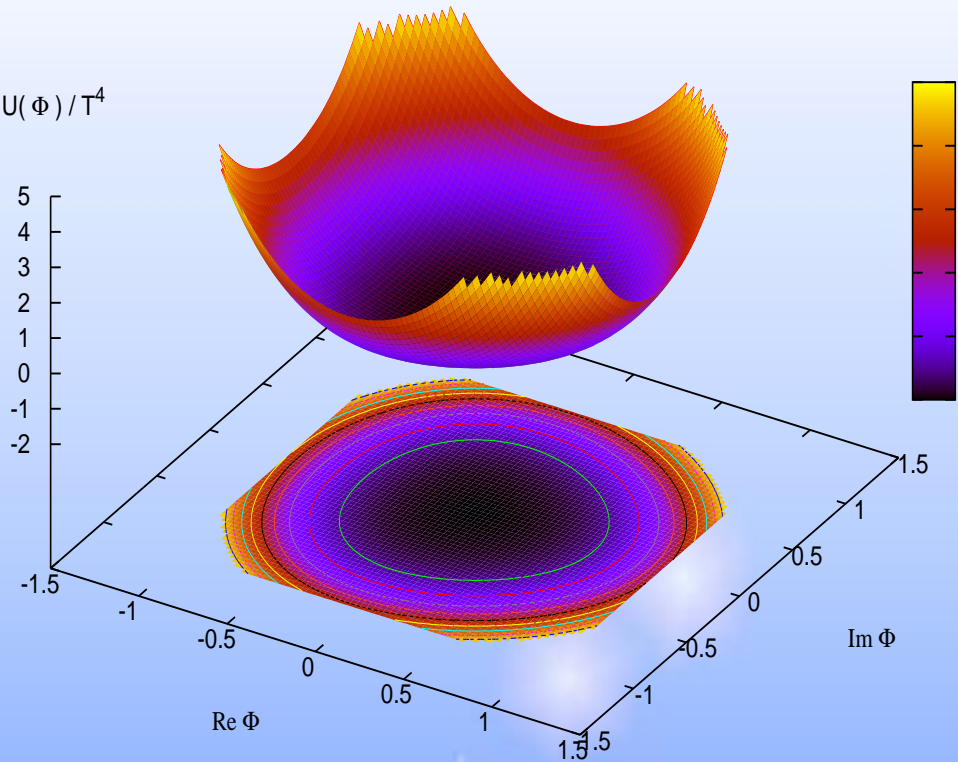
In the following $\mathcal{U}(\Phi[A], \bar{\Phi}[A]; T)$ can also be chosen in its logarithmic form.



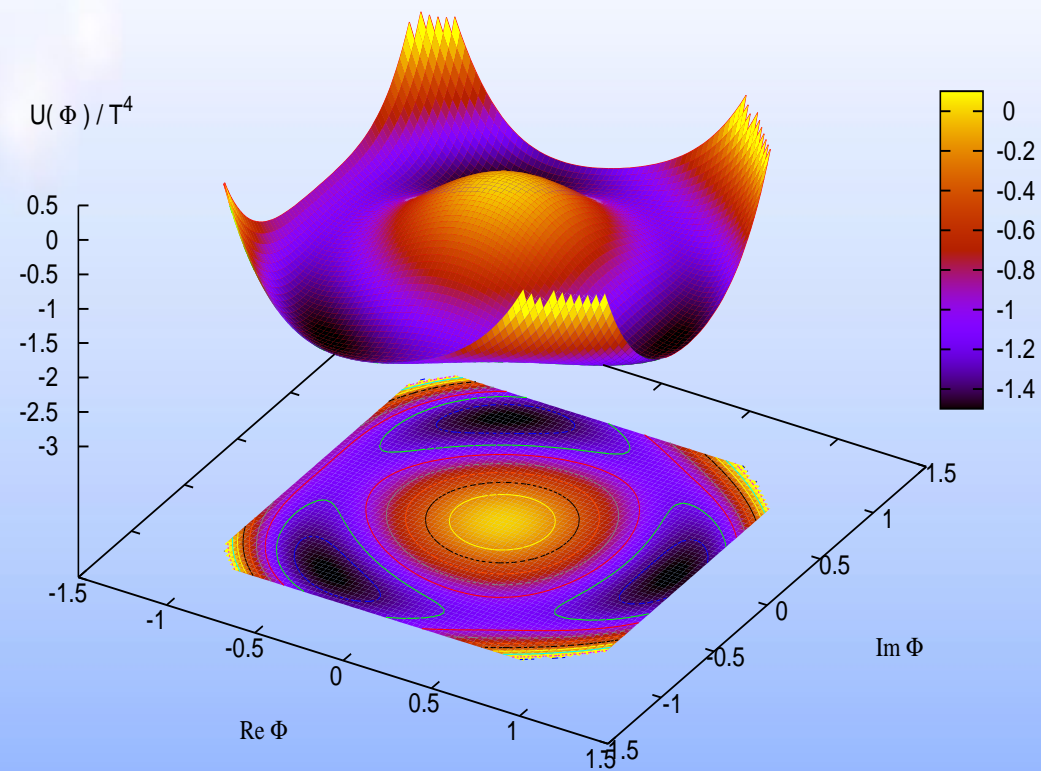
C. Ratti, M. Thaler, W. Weise, hep-ph/0604025 :
lattice: O. Kaczmarek, F. Karsch, P. Petreczky,
F. Zantow, Phys. Lett. B 543, 41 (2002).

Pure gauge sector: the effective potential $\mathcal{U}(\Phi, \bar{\Phi}; T)$

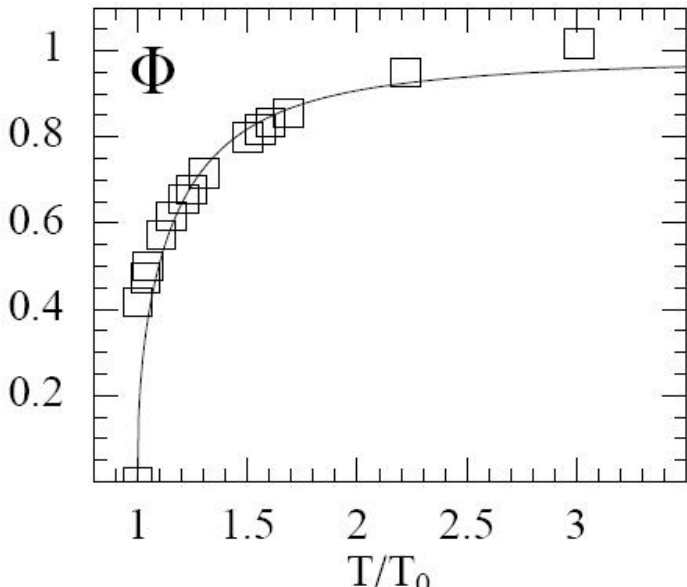
$T < T_0$
 Color “confinement”
 $\langle \Phi \rangle = 0 \longrightarrow$ no \mathbb{Z}_3 breaking



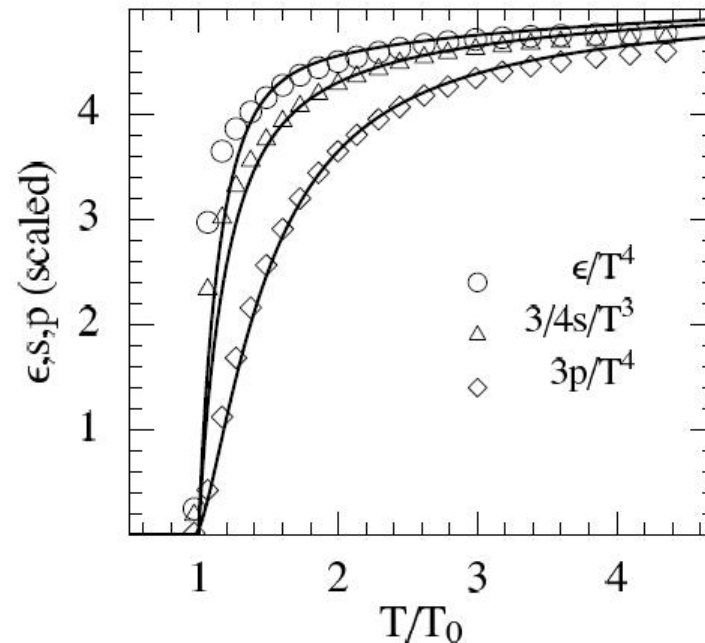
$T > T_0$
 Color “deconfinement”
 $\langle \Phi \rangle \neq 0 \longrightarrow \mathbb{Z}_3$ broken



Lattice results (pure gauge)



(a)



(b)

(a): Polyakov loop (Lattice : O. Kaczmarek, F. Karsch, P. Petreczky, and F. Zantow, Phys. Lett. B **543**, 41 (2002)). (b): Pressure, entropy and energy density (scaled) (Lattice : G. Boyd *et al.*, Nucl. Phys. B **469**, 419 (1996)).

Claudia Ratti, Michael A. Thaler, Wolfram Weise, Phys.Rev.D73:014019,2006, hep-ph/0506234

a_0	a_1	a_2	a_3	b_3	b_4
6.75	-1.95	2.625	-7.44	0.75	7.5

Schwinger–Dyson equations at the Hartree level

* Hartree approximation:

Calculation of the quasi-quark Hartree propagator $\mathcal{S}(p_n = i\omega_n, \vec{p})$,

quadri-momentum $p = (p_n, \vec{p})$ with $p_n = i\omega_n$

and $\omega_n = (2n + 1)\pi T$ (Matsubara frequency for a fermion)

Free propagator in the background field A_4 : $\text{——} = -(\not{p} - m_0 + \gamma^0(\mu - iA_4))^{-1}$

$\times = \Gamma_M$, $M = \{\text{Scalar}, \text{Pseudoscalar}\}$ $\Gamma_S \equiv \mathbb{I}$, $\Gamma_P^a \equiv i\gamma_5\tau^a$

• $\equiv 2G_1$: coupling constant in the scalar-pseudoscalar channel

$$\mathcal{S}^{-1} = \text{——} = \text{——} + \text{——} \circlearrowleft \Sigma \text{——} \quad (\text{Schwinger-Dyson equation})$$

$$\mathcal{S}^{-1} \simeq \text{——} + \text{——} \circlearrowleft = -(\not{p} - m + \gamma^0(\mu - iA_4))^{-1}$$

with $\circlearrowleft \Sigma_H = \circlearrowleft \equiv m - m_0$

$$m - m_0 = 2G_1 \text{Tr}_{c,f,D} \sum_{n=-\infty}^{+\infty} T \int_{\Lambda} \frac{d^3 p}{(2\pi)^3} \frac{-1}{\not{p} - m + \gamma^0(\mu - iA_4)}$$

(self-consistency condition defining the Hartree equation)

Mean field equations

✿ Grand potential at finite temperature and density

The solutions of the (mean) field equation at finite temperature and density are obtained by minimizing the effective grand potential.

$$\begin{aligned}\Omega &= \mathcal{U}(\Phi, \bar{\Phi}, T) + \frac{(m - m_0)^2}{2G_1} - 6N_f \int_{\Lambda} \frac{d^3 p}{(2\pi)^3} E_p \\ &\quad - 2N_f T \int_{\Lambda} \frac{d^3 p}{(2\pi)^3} \left\{ \text{Tr}_c \ln \left[1 + \mathbf{L} e^{-(E_p - \mu)/T} \right] + \text{Tr}_c \ln \left[1 + \mathbf{L}^\dagger e^{-(E_p + \mu)/T} \right] \right\}\end{aligned}$$

$E_p = \sqrt{\vec{p}^2 + m^2}$: single Hartree quasi-particle energy (or constituent quark mass).

With $\beta = 1/T$,

$$\begin{aligned}\text{Tr}_c \ln \left[1 + \mathbf{L} e^{-(E_p - \mu)/T} \right] &= \ln \left[1 + 3\Phi e^{-\beta(E_p - \mu)} + 3\bar{\Phi} e^{-2\beta(E_p - \mu)} + e^{-3\beta(E_p - \mu)} \right] \\ \text{Tr}_c \ln \left[1 + \mathbf{L}^\dagger e^{-(E_p + \mu)/T} \right] &= \ln \left[1 + 3\bar{\Phi} e^{-\beta(E_p + \mu)} + 3\Phi e^{-2\beta(E_p + \mu)} + e^{-3\beta(E_p + \mu)} \right] \\ \lim_{\Phi, \bar{\Phi} \rightarrow 0} (\mathbb{Z}_3 \text{ restored}) &= \ln \left[1 + e^{-3\beta(E_p + \mu)} \right] \\ \lim_{\Phi, \bar{\Phi} \rightarrow 1} (\mathbb{Z}_3 \text{ broken}) &= N_c \ln \left[1 + e^{-\beta(E_p + \mu)} \right]\end{aligned}$$

From NJL to PNJL

Summations over Matsubara frequencies:

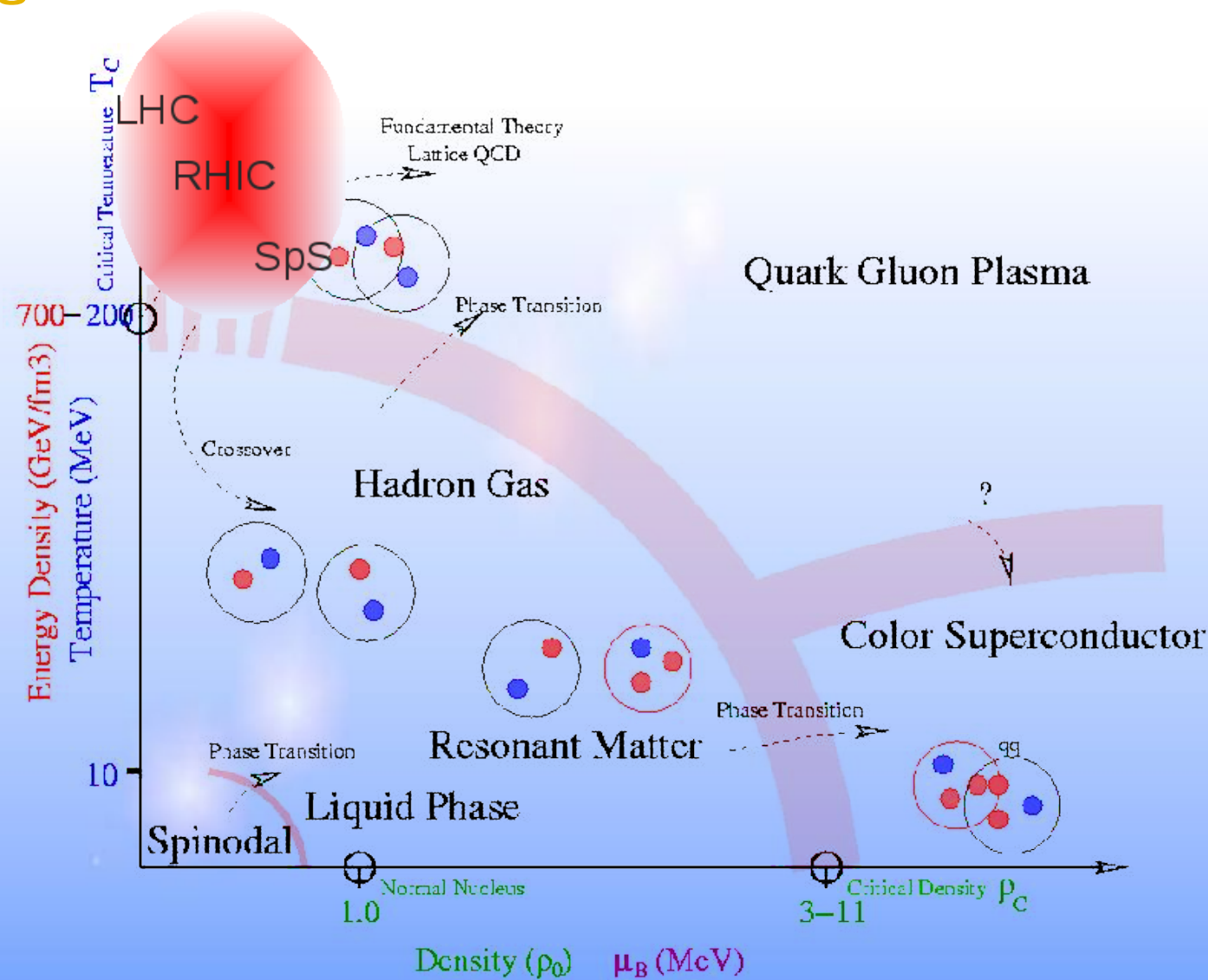
$$\text{Tr}_c F(E_p - \mu - iA_4) \equiv T \sum_n \text{Tr} \frac{1}{i\omega_n - E_p + \mu + iA_4} = -T \frac{\partial z_A^+}{\partial E_p}$$

with $z_A^+ \equiv \ln \left(1 + L e^{-\beta(E_p - \mu)} \right)$ (for the case $F(E_p + \mu + iA_4)$ one uses $z_A^- \equiv \ln \left(1 + L^\dagger e^{-\beta(E_p + \mu)} \right)$)

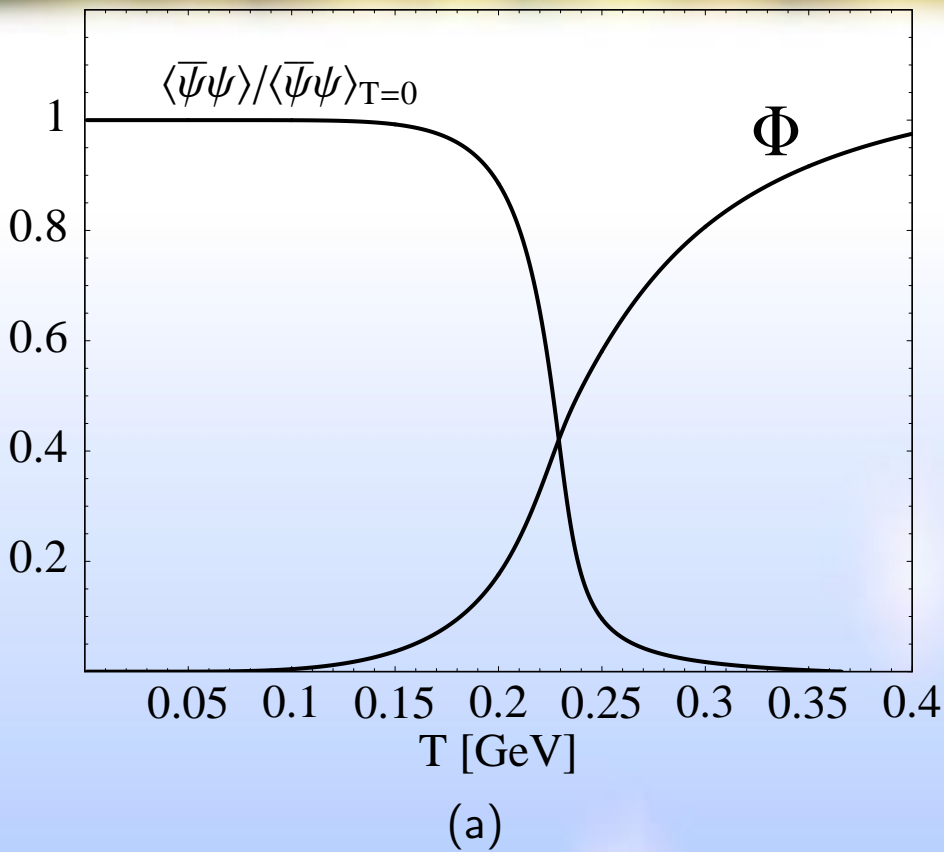
$$\begin{aligned} f(E_p - \mu) &= \frac{1}{1 + e^{\beta(E_p - \mu)}} \implies f_\Phi^+(E_p) \equiv \frac{1}{N_c} \text{Tr}_c F(E_p - \mu - iA_4) \\ f_\Phi^+(E_p) &= \frac{\left(\Phi + 2\bar{\Phi}e^{-\beta(E_p - \mu)} \right) e^{-\beta(E_p - \mu)} + e^{-3\beta(E_p - \mu)}}{1 + 3 \left(\Phi + \bar{\Phi}e^{-\beta(E_p - \mu)} \right) e^{-\beta(E_p - \mu)} + e^{-3\beta(E_p - \mu)}} \\ f(E_p + \mu) &= \frac{1}{1 + e^{\beta(E_p + \mu)}} \implies f_\Phi^-(E_p) \equiv \frac{1}{N_c} \text{Tr}_c F(E_p + \mu + iA_4) \\ f_\Phi^-(E_p) &= \frac{\left(\bar{\Phi} + 2\Phi e^{-\beta(E_p + \mu)} \right) e^{-\beta(E_p + \mu)} + e^{-3\beta(E_p + \mu)}}{1 + 3 \left(\Phi + \bar{\Phi}e^{-\beta(E_p + \mu)} \right) e^{-\beta(E_p + \mu)} + e^{-3\beta(E_p + \mu)}} \end{aligned}$$

Part II:

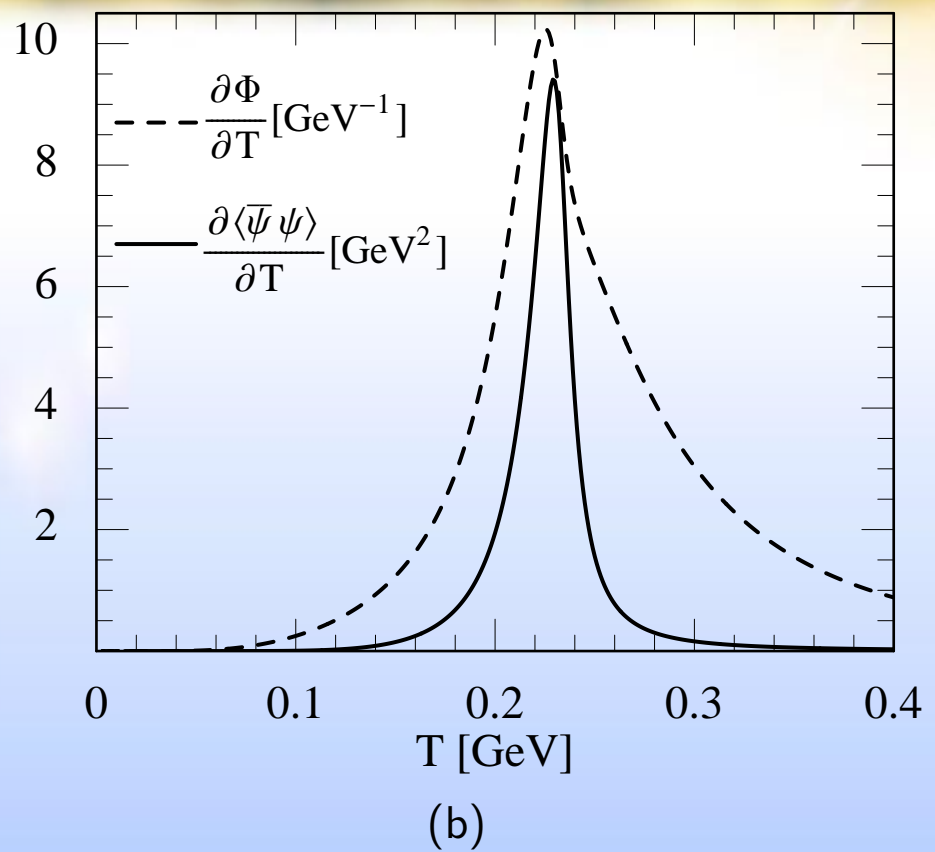
Phase diagram: critical behavior



Chiral crossover and deconfinement: mean field results for $\mu = 0$



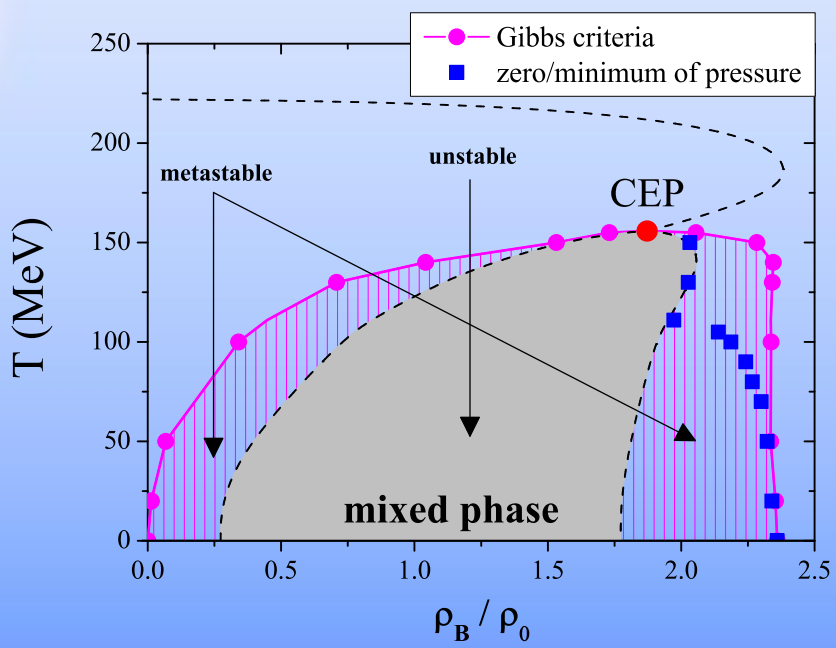
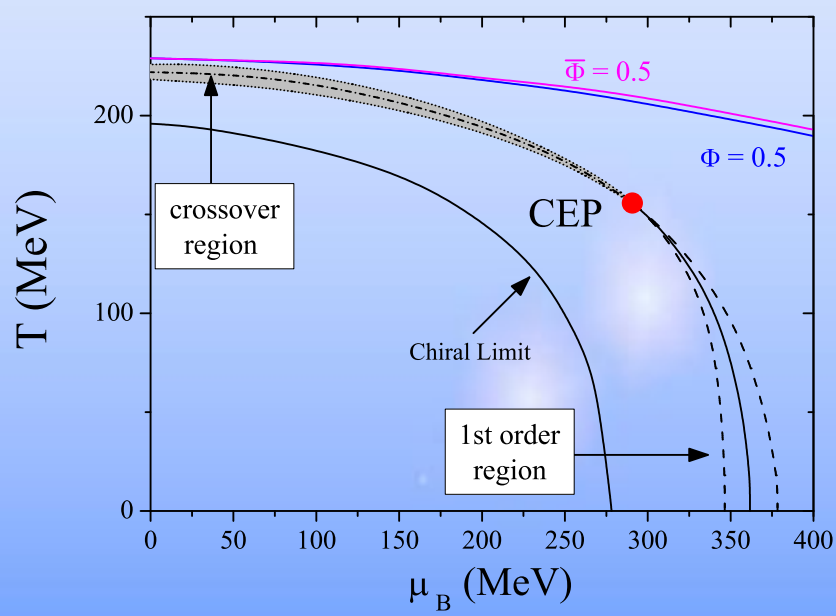
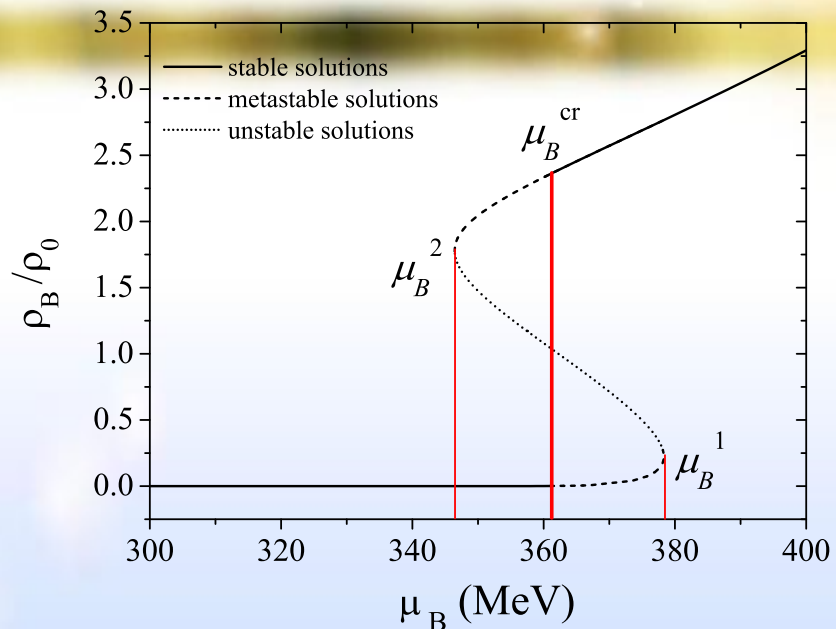
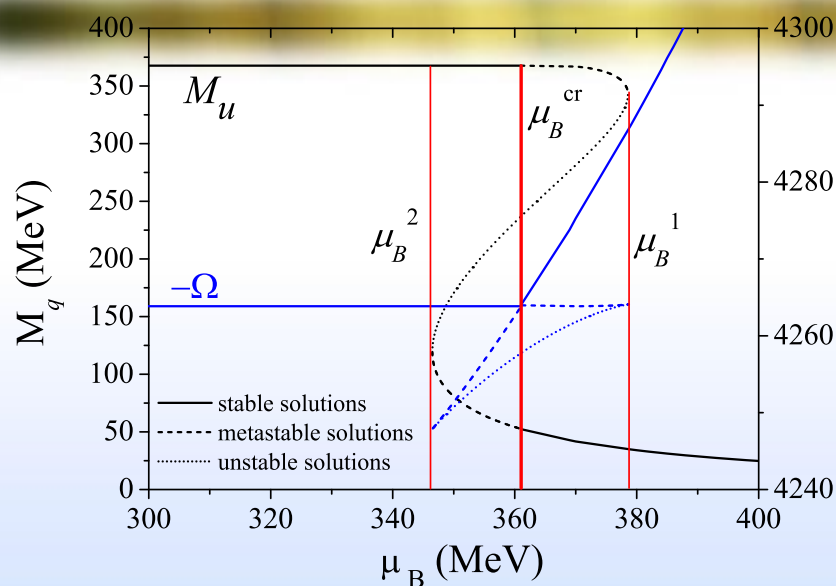
(a)



(b)

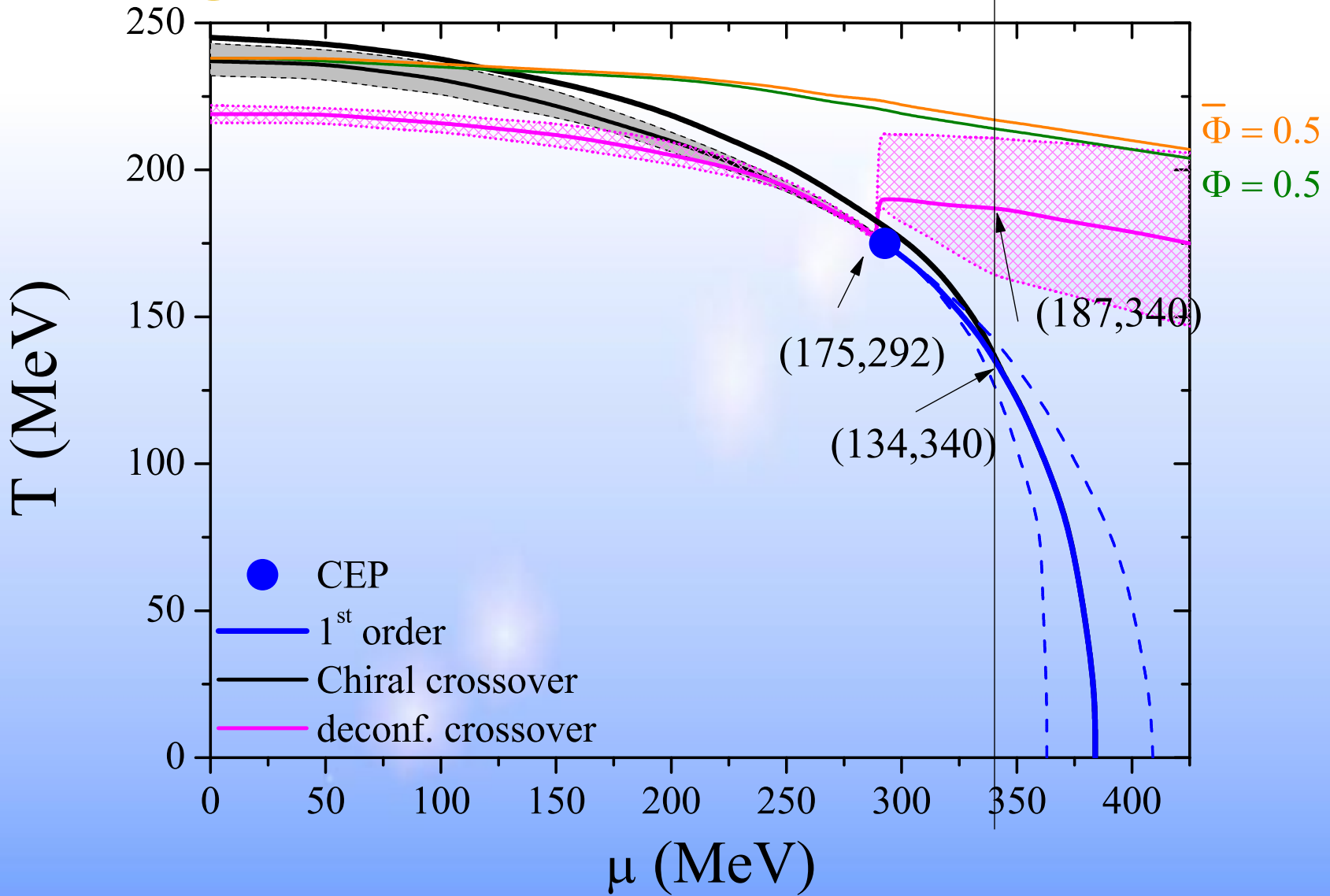
Left: scaled chiral condensate and Polyakov loop $\Phi(T)$ as functions of temperature at zero chemical potential. Right: plots of $\partial \langle \bar{\psi} \psi \rangle / \partial T$ and $\partial \Phi / \partial T$. Notice that the Φ “bump” is larger and assymetric (left side looks like the chiral one)

Metastability (SU(3))

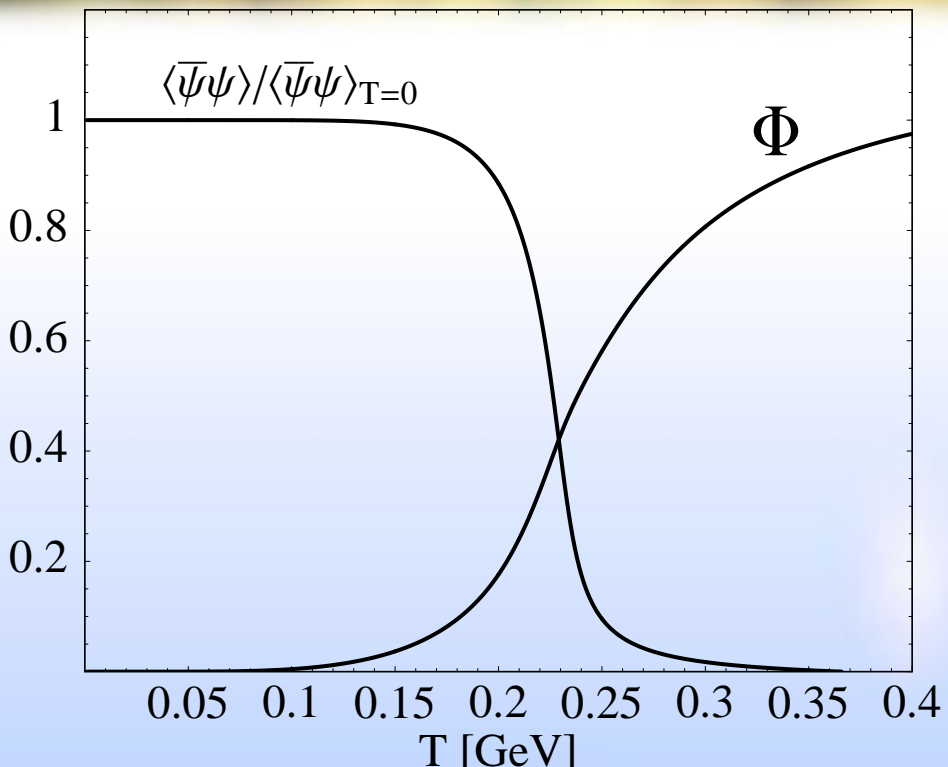


Part III: Confined Chirality Symmetric phase

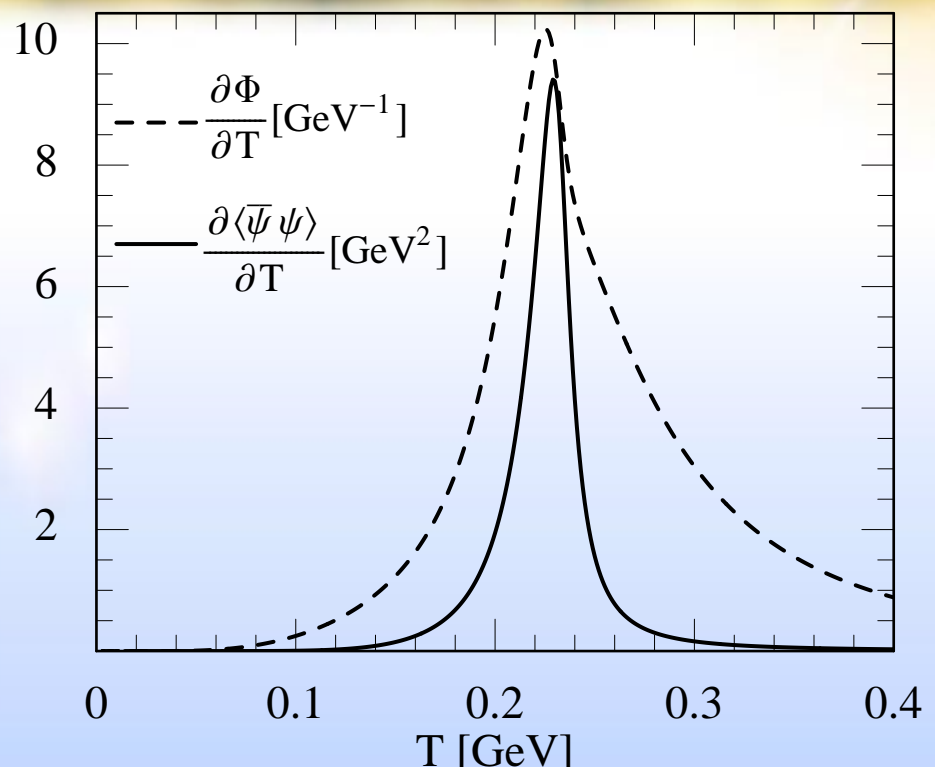
Exploring the CCS phase with mesonic correlations



Chiral crossover and deconfinement: mean field results for $\mu = 0$



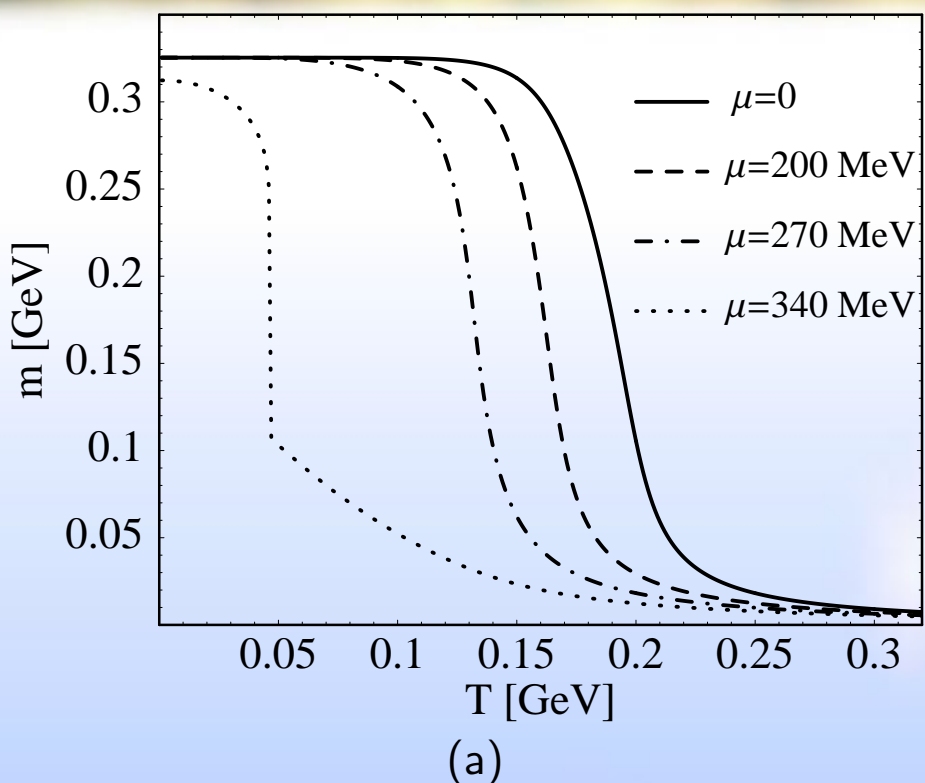
(a)



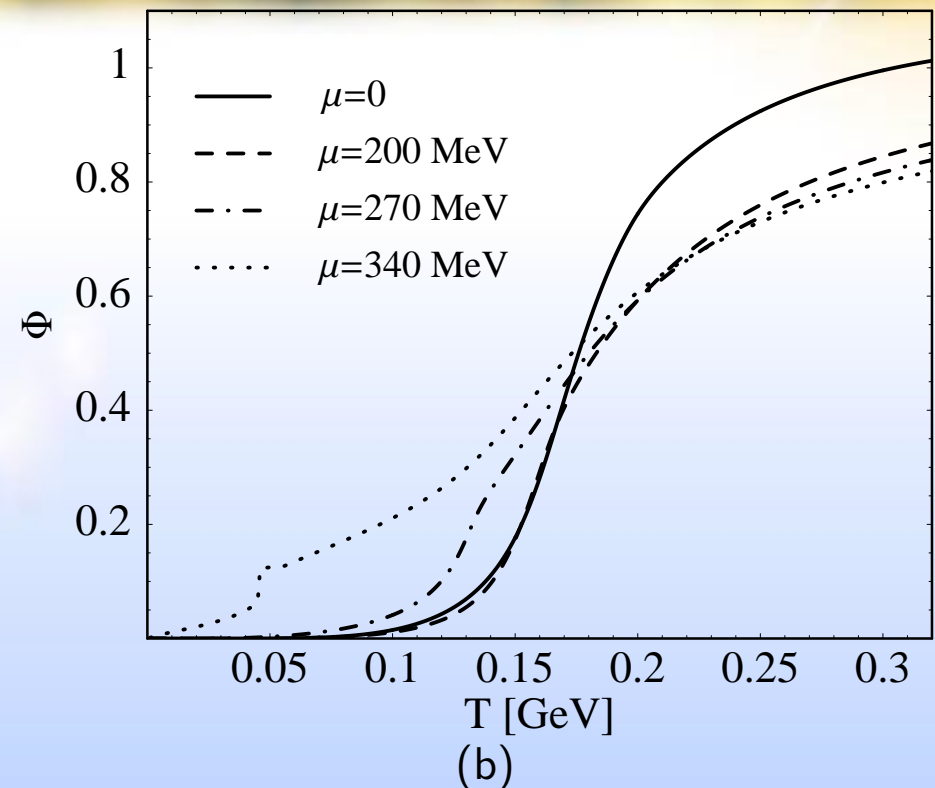
(b)

Left: scaled chiral condensate and Polyakov loop $\Phi(T)$ as functions of temperature at zero chemical potential. Right: plots of $\partial \langle \bar{\psi} \psi \rangle / \partial T$ and $\partial \Phi / \partial T$. Notice that the Φ “bump” is larger and assymetric (left side looks like the chiral one)

Mean field results: $\mu \neq 0$



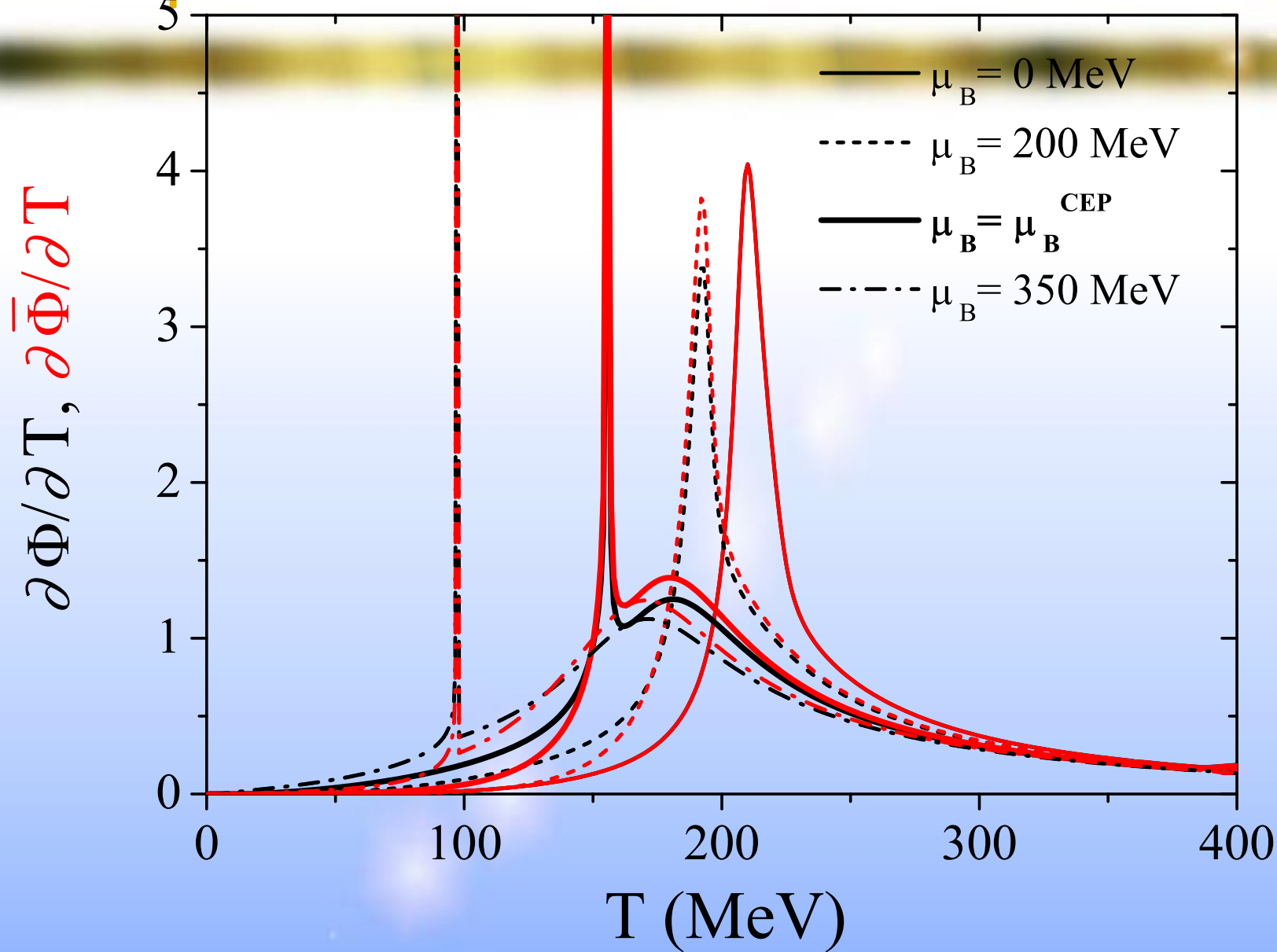
(a)



(b)

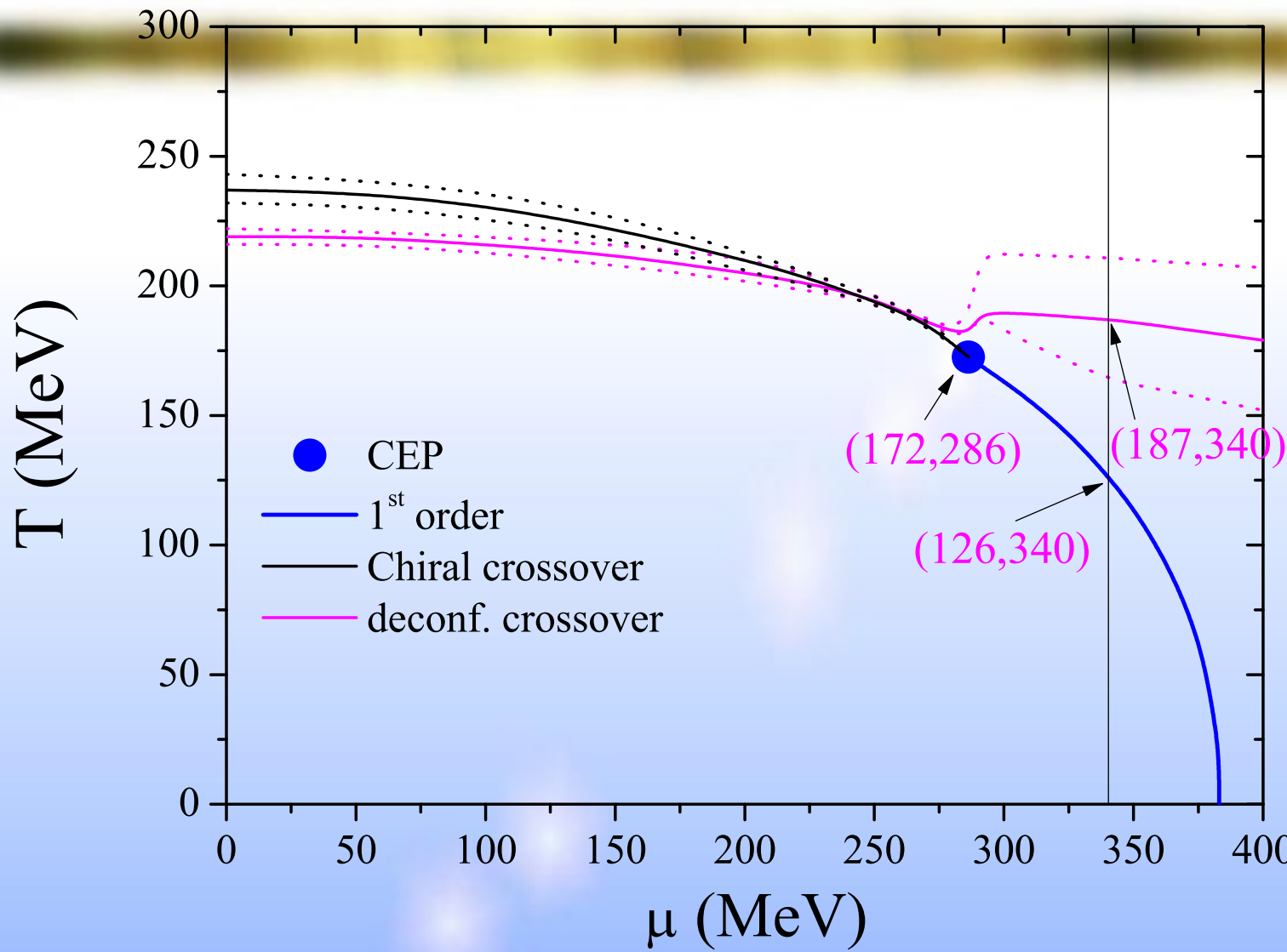
Constituent quark mass (a) and Polyakov loop (b) as functions of temperature for different values of the chemical potential.

Order parameter: mean field calculation



Influence of the chiral transition on Φ : dissymmetry of the bump that is decoupling at high chemical potential.

Order parameter: mean field calculation



Mean field evidence of the opening of a CCS phase at the CEP
⇒ How does mesons look like in this phase ?

Schwinger–Dyson equations at the Hartree+RPA level

* **Hartree approximation:** $\left\{ \begin{array}{l} \times = \Gamma_M, M = \{S, P\}, \Gamma_S \equiv \mathbb{I}, \Gamma_P^a \equiv i\gamma_5\tau^a \\ \bullet \equiv 2G_1: \text{coupling constant} \end{array} \right.$

$$\mathcal{S}^{-1} \simeq \text{---} + \text{---} \circlearrowleft, \left(\text{---} \overset{\Sigma}{\underset{H}{\circlearrowleft}} \right) = \text{---} \circlearrowright \equiv m - m_0$$

$$\left. \begin{array}{l} p = (p_0, \vec{p}) \rightarrow (i\omega_n + \mu - iA_4, \vec{p}) \\ i \int_{\Lambda} \frac{d^4 p}{(2\pi)^4} \rightarrow -T \frac{1}{N_c} \text{Tr}_c \sum_n \int_{\Lambda} \frac{d^3 p}{(2\pi)^3} \end{array} \right\} m - m_0 = i2G_1 N_c \text{Tr}_{f,D} \int_{\Lambda} \frac{d^4 p}{(2\pi)^4} \frac{1}{\not{p} - m}$$

* **RPA (ring) :** Correlators of current operators carrying the quantum numbers of physical mesons.

$$C^{MM}(q^2) \equiv i \int d^4x e^{iq.x} \left\langle 0 \left| T \left(J_M(x) J_M^\dagger(0) \right) \right| 0 \right\rangle = \text{---} \circlearrowleft \text{---} \text{C}$$

$$\left. \begin{array}{l} J_P^a(x) = \bar{q}(x) i\gamma_5\tau^a q(x) \quad (\text{pseudoscalar isovector current: pion}) \\ \Rightarrow \Pi_{ab}^{PP}(q^2) = \int_{\Lambda} \frac{d^4 p}{(2\pi)^4} \text{Tr} i\gamma_5\tau^a S(p+q) i\gamma_5\tau^b S(q) \\ J_S(x) = \bar{q}(x) q(x) - \langle \bar{q}(x) q(x) \rangle \quad (\text{scalar isoscalar current: sigma}) \\ \Rightarrow \Pi^{SS}(q^2) = \int_{\Lambda} \frac{d^4 p}{(2\pi)^4} \text{Tr} S(p+q) S(q) \end{array} \right\} \text{---} \circlearrowright \text{---} \Pi$$

$$\text{---} \text{C} \simeq * \text{---} \Pi * + * \text{---} \Pi * \text{---} \text{C} \Rightarrow C^{MM}(q^2) \frac{\Pi^{MM}(q^2)}{1 - 2G_1 \Pi^{MM}(q^2)} \text{ (ring approximation)}$$

Spectral function

The spectral function F^{MM} of the correlator C^{MM} is:

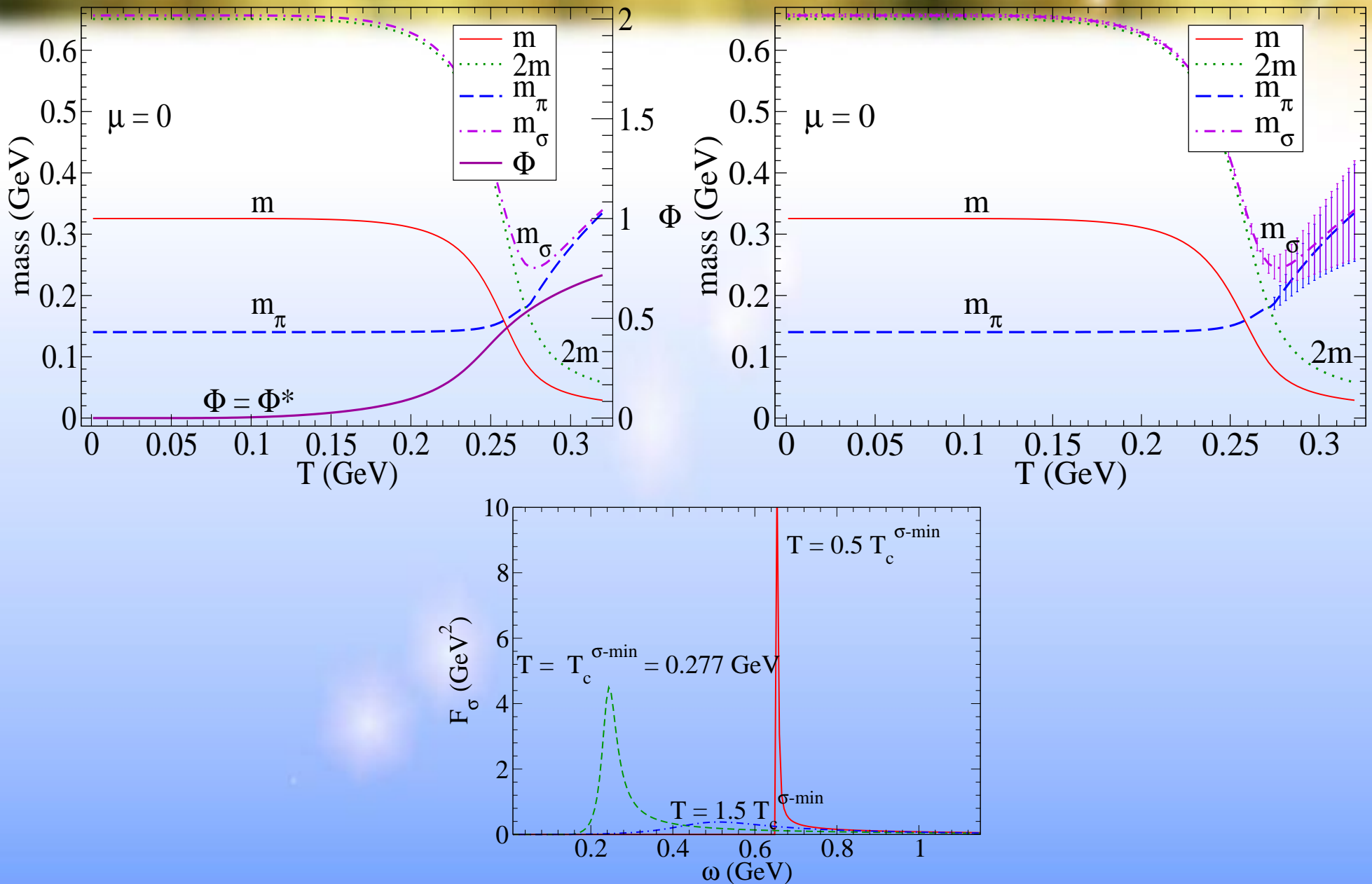
$$F^{MM}(\omega, \vec{q}) \equiv \Im m C^{MM} = \Im m \frac{\Pi^{MM}}{1 - 2G_1\Pi^{MM} - i\varepsilon}$$

In particular at $\vec{q} = 0$, $\omega < 2m$ and $\Im m I_2 = 0$:

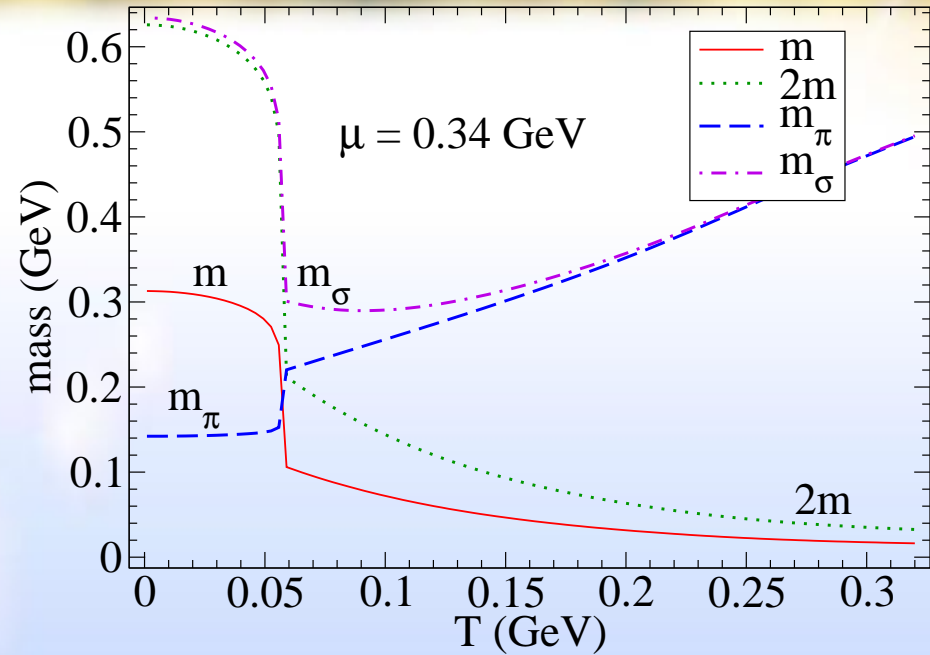
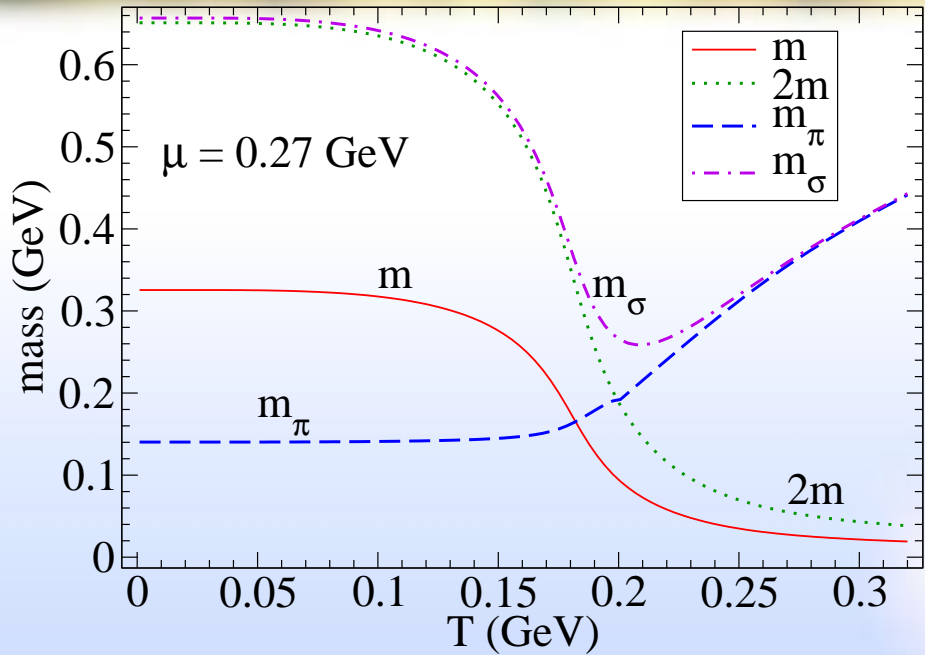
$$F^{MM}(\omega) = \frac{\pi}{2G_1} \delta \left(1 - 2G_1\Pi^{MM}(\omega) \right).$$

The spectral function has a Dirac peak at the meson mass ; the disintegration channel $M \rightarrow q\bar{q}$ is closed. If the mass is above $2m$, the meson has a width due to the decay into two quarks because NJL or PNJL models do not confine really the quarks.

PNJL masses and spectral functions for π and σ , $\mu = 0$

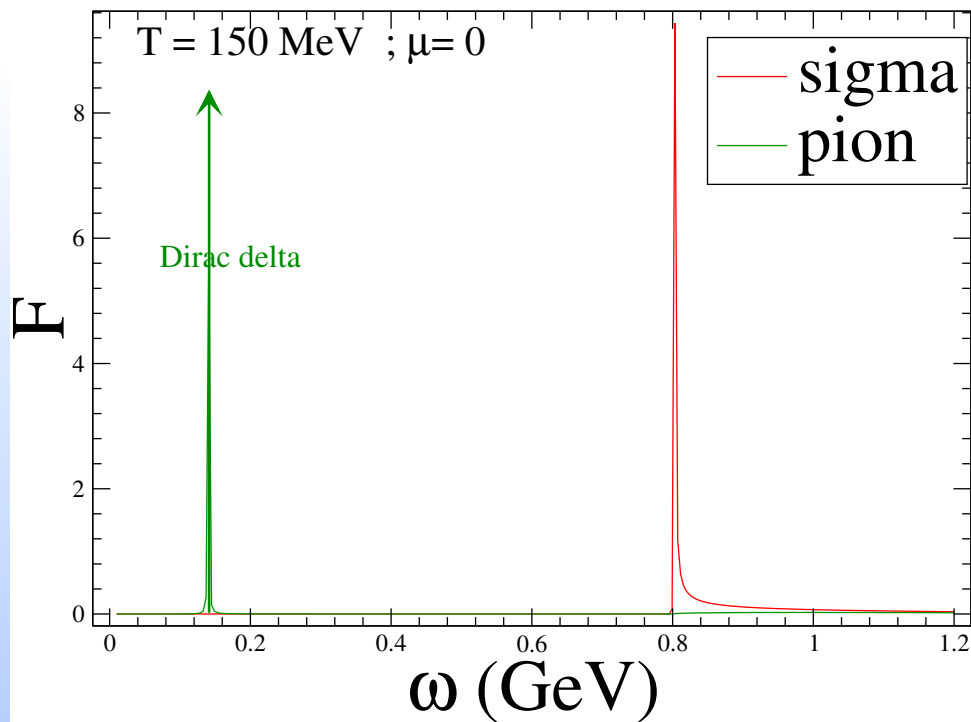


Meson masses, $\mu = 0.27 \text{ GeV}$ et $\mu = 0.34 \text{ GeV}$



Mesonic spectral functions as a probe of the phase properties

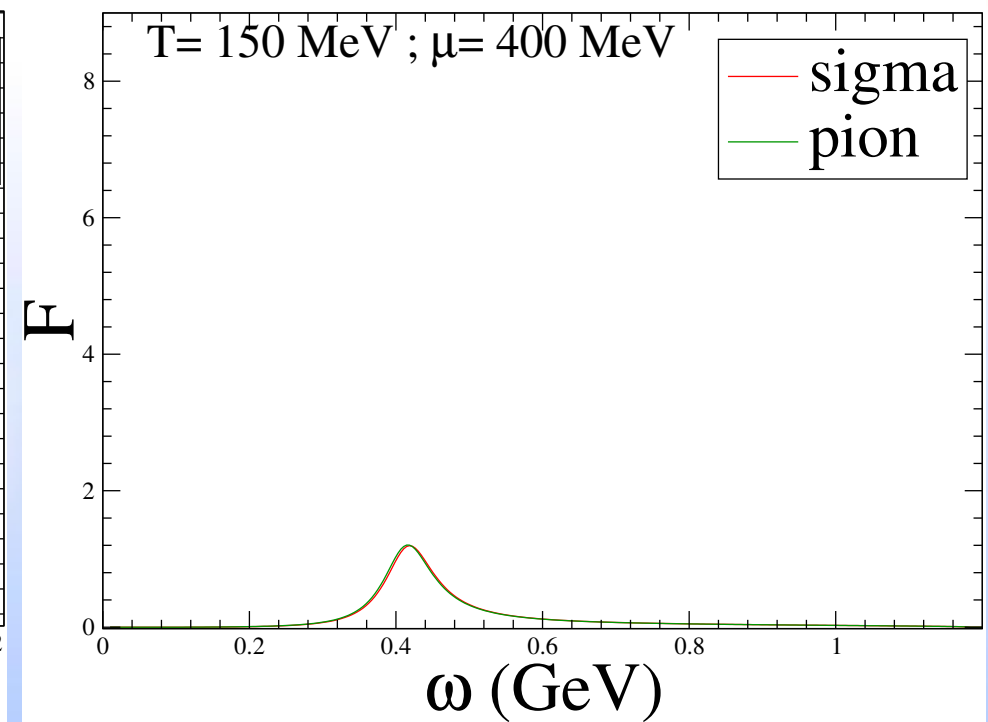
Spectral functions



Confining regime: σ is a narrow resonance ;
chiral symmetry broken

$$\langle \bar{q}q \rangle \neq 0 ; \Phi \simeq 0$$

Spectral functions

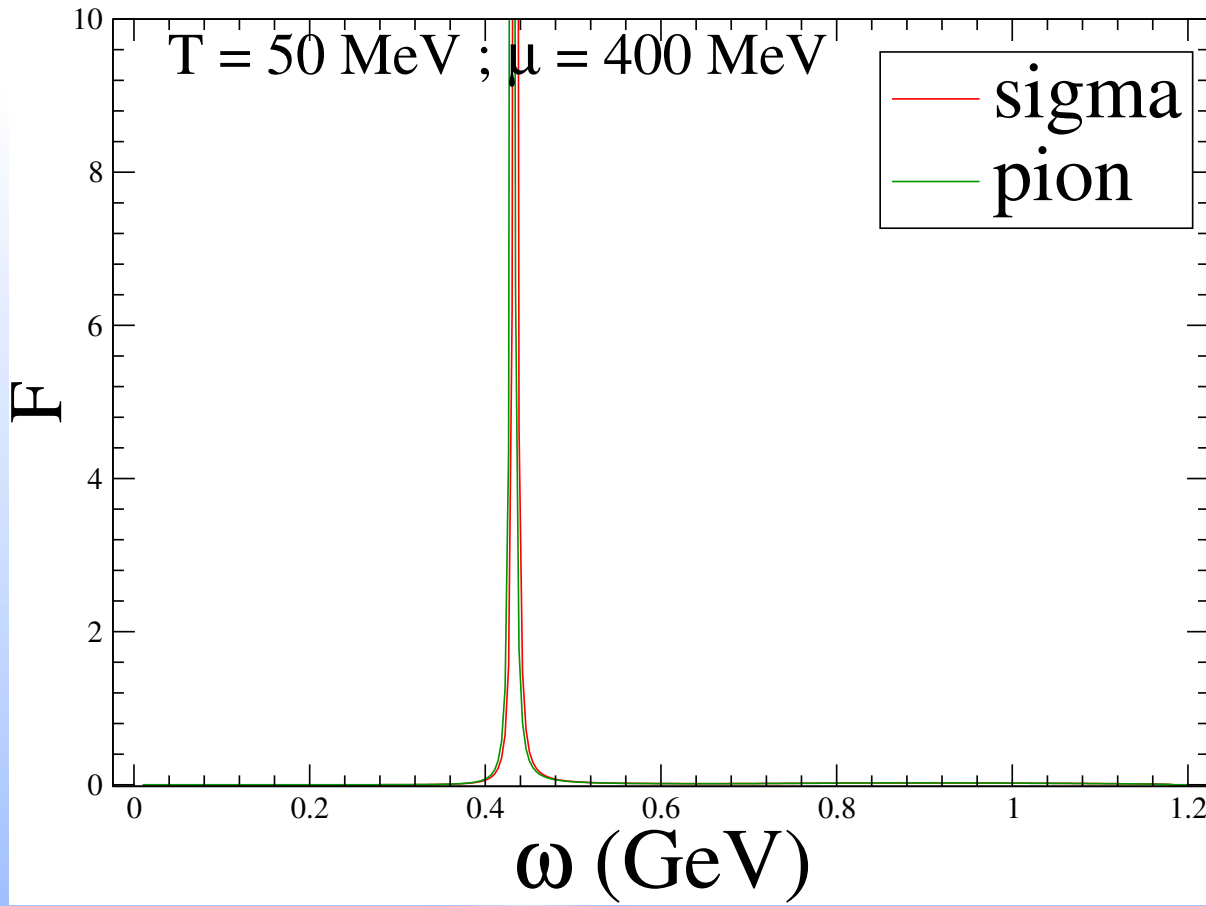


Deconfinement: σ and π spectral function are almost the same as an uncorrelated $\bar{q}q$ pair ;
chiral symmetry restored

$$\langle \bar{q}q \rangle \simeq 0 ; \Phi \neq 0$$

Mesonic spectral functions as a probe of the phase properties

Spectral functions



$$\langle \bar{q}q \rangle \simeq 0 ; \Phi \simeq 0$$

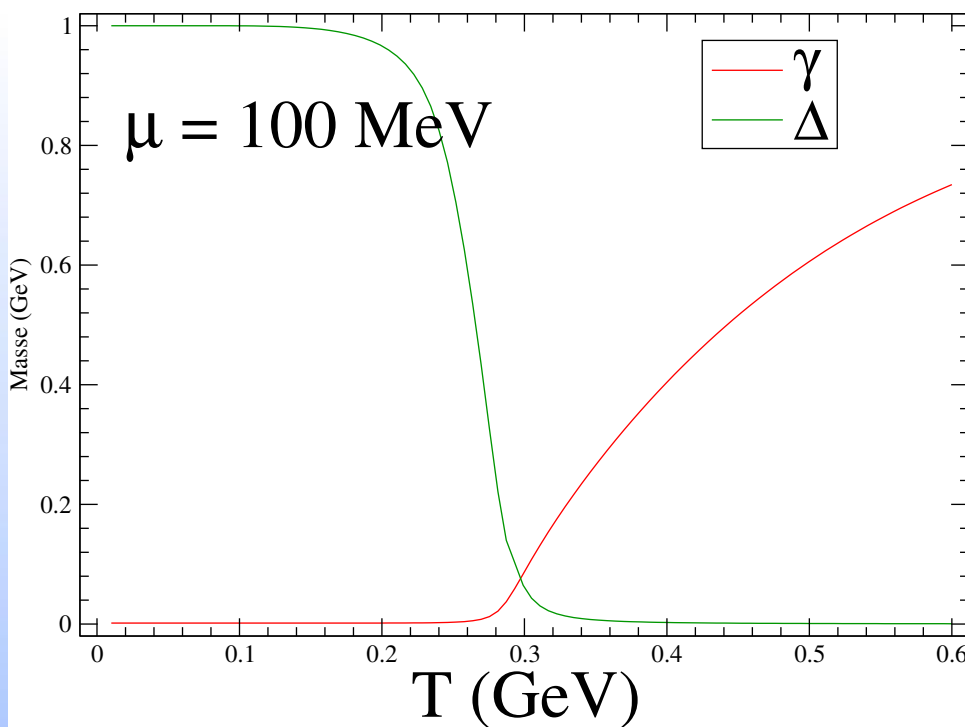
“Confining” regime: σ and π are still narrow resonances ; chiral symmetry restored

⇒ the PNJL Confined Chirally Symmetric (quarkyonic) phase really changes mesonic modes propagation

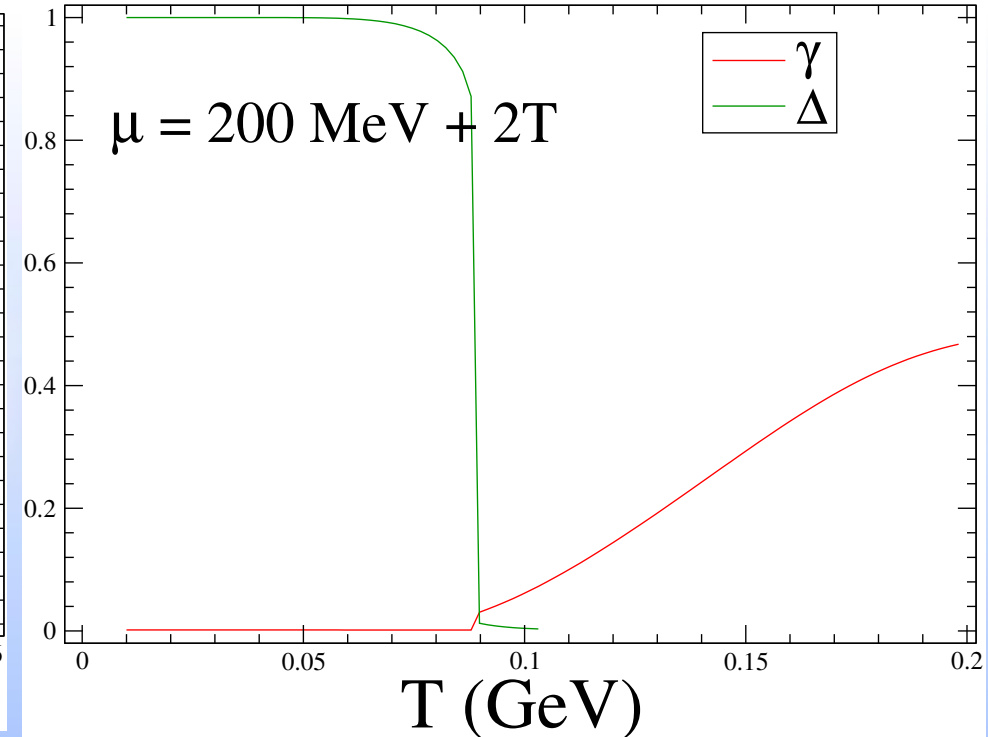
Mesonic order-like parameters

Chiral restoration: $m_\sigma - m_\pi$ (normalized at one in the vacuum) $\rightarrow \Delta$

Deconfinement: $\gamma = \Gamma_\sigma/\Lambda = \text{decay width } (\sigma \rightarrow \bar{q}q)$



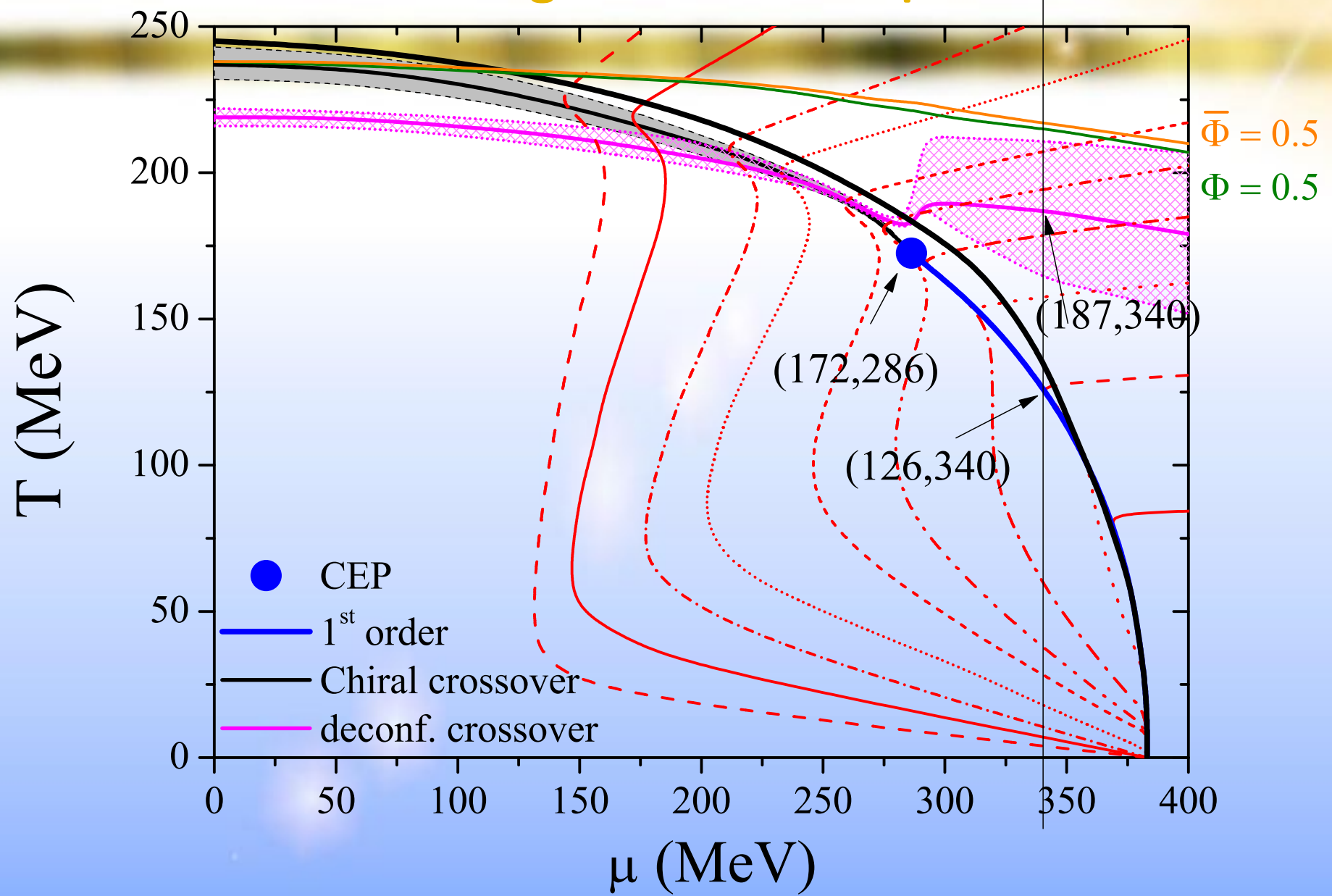
Fast deconfinement (as soon as chiral symmetry is restored)



Slower deconfinement ; inflexion point is moved to higher temperature

PNJL has no confinement mechanism but the “breaking” of confinement is small in the vacuum: the model may be used to discuss such features.

As a conclusion: Phase diagram and isentropic lines



Conclusions

More and more effective models that use inputs from lattice QCD → interpretation and extension of LQCD results:

- PNJL and PQM models class
- LQCD Gluon propagator plugged in a NJL model (P.Costa, O.Oliveira, P.J.Silva)

- The PNJL reproduces well at the mean field level the lattice calculations.
- PNJL calculations can be directly deduced from NJL ones (not only for one loop calculation, but to all orders) by a redefinition of the usual Fermi – Dirac distribution function.
- PNJL results does not destroy the important features like chiral restauration, Goldstone character of the pion, etc.
- The introduction of gluons in NJL via a background temporal gauge field embedded in the Polyakov loop add some statistical confinement to the NJL model. No mechanism for true confinement in PNJL ; yet The results are improved in the right direction (quarks more “bounded” in meson below T_c and less bound above T_c) compared to NJL.

- Elongation of the critical region in the PNJL model ; mean field critical exponents are obtained.
- Effects of the TCP on the CEP are seen.

- Exploration of the quarkyonic phase: the mesonic correlations are sensitive to this regime.
- PNJL is a pertinent model to discuss confinement / deconfinement properties.

BACKUP SLIDES

2

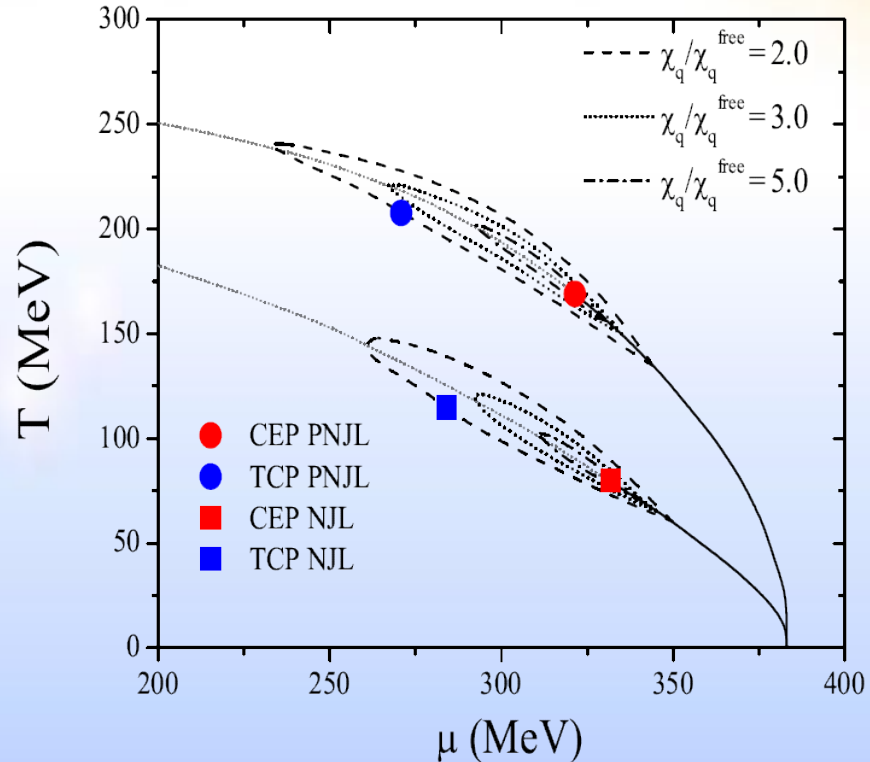
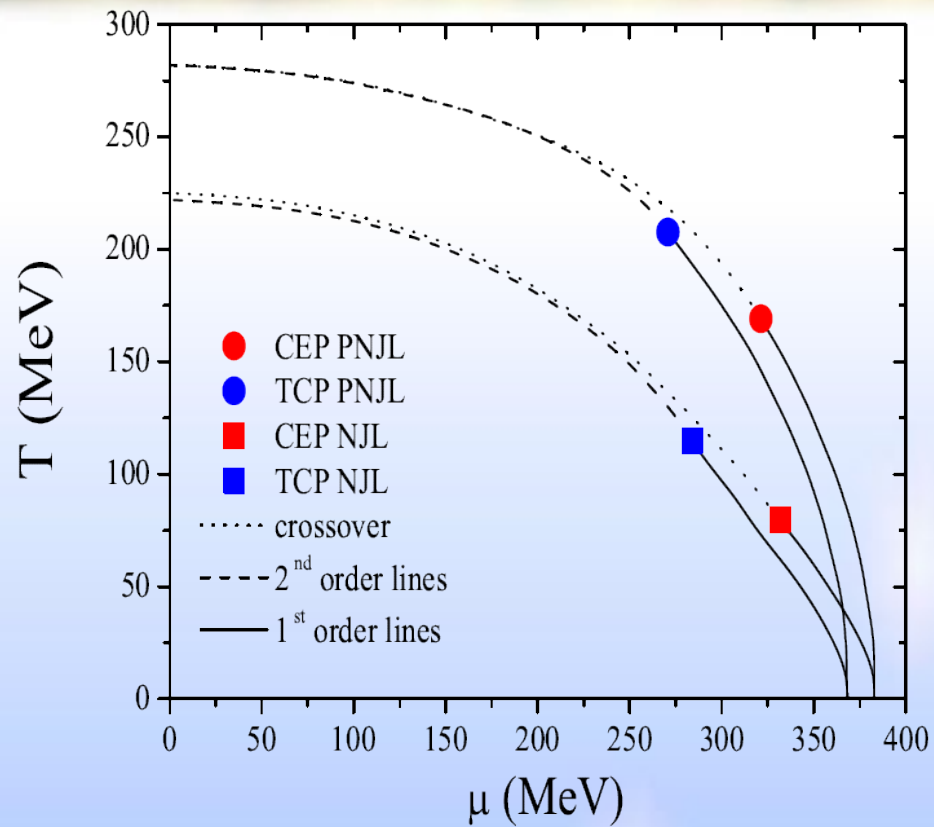
Baryon number susceptibility and specific heat

The baryon number susceptibility and the specific heat are the response of the baryon number density $\rho_q(T, \mu)$ and the entropy $S(T, \mu)$ to an infinitesimal variation of the quark chemical potential μ and temperature, given respectively by:

$$\chi_q = \left(\frac{\partial \rho_q}{\partial \mu} \right)_T, \quad \text{and} \quad C = \frac{T}{V} \left(\frac{\partial S}{\partial T} \right)_\mu.$$

The baryon number density is given by $\rho_q = \frac{N_c}{\pi^2} \int p^2 dp (f_\Phi(\mu, T) - \bar{f}_\Phi(\mu, T))$ where $f_\Phi(\mu, T)$ and $\bar{f}_\Phi(\mu, T)$ are the occupation numbers modified by the Polyakov loop.

Phase diagram and critical region

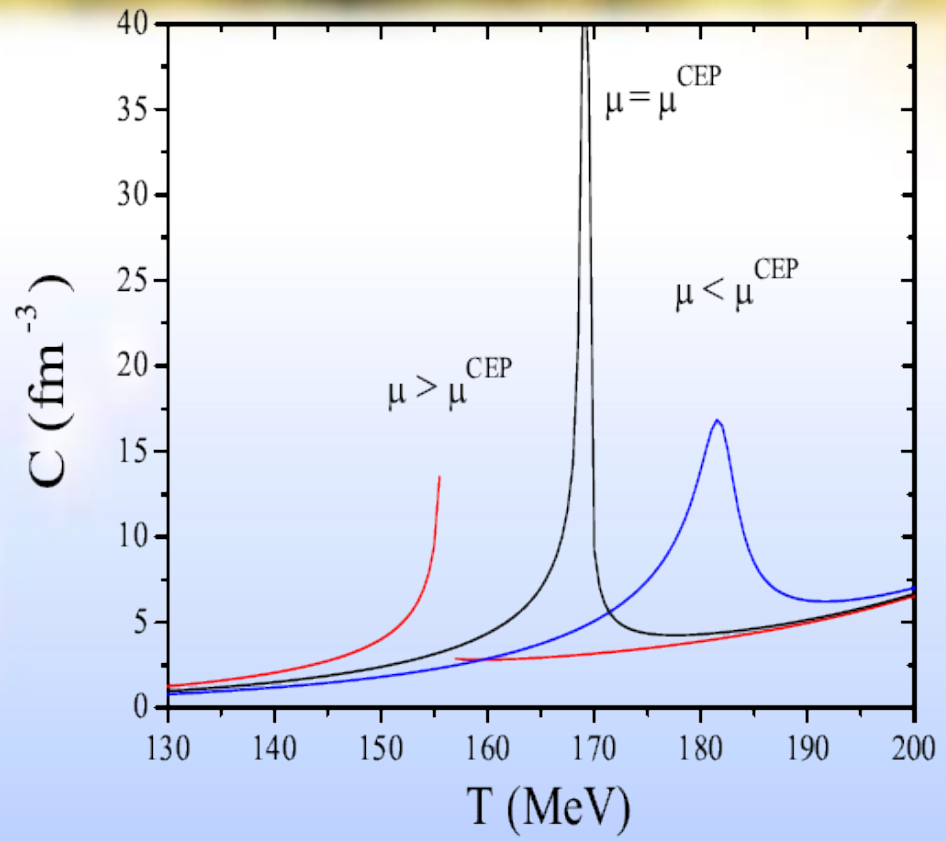
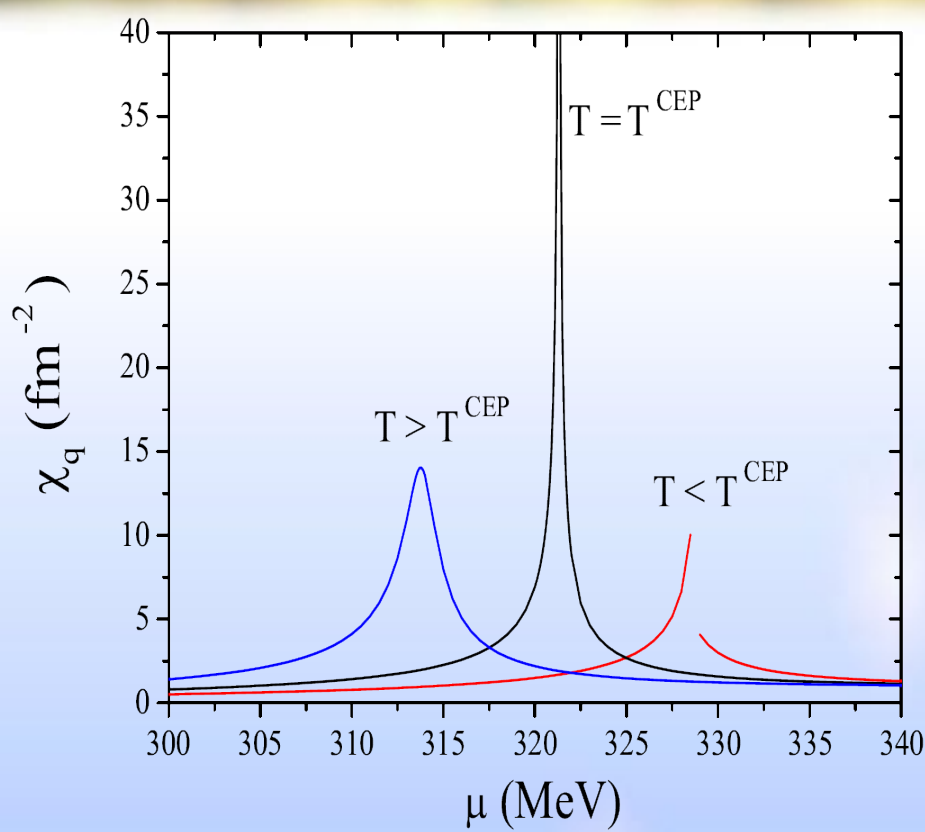


	T^{CEP}	μ^{CEP}
PNJL	169.11 MeV	321.32 MeV
NJL	79.92 MeV	331.72 MeV

	T^{TCP}	μ^{TCP}
PNJL	207.66 MeV	270.80 MeV
NJL	112.08 MeV	286.05 MeV

The CEP in the PNJL model is closer to lattice results (Karsh, hep-lat/0601013 and Fodor and Katz, J. High Energy Phys. 0204 (2004), 050) ; the main change with regards to NJL values is in T^{CEP} and T^{TCP} (the effects of the inclusion of the Polyakov loop are more relevant in the temperature direction).

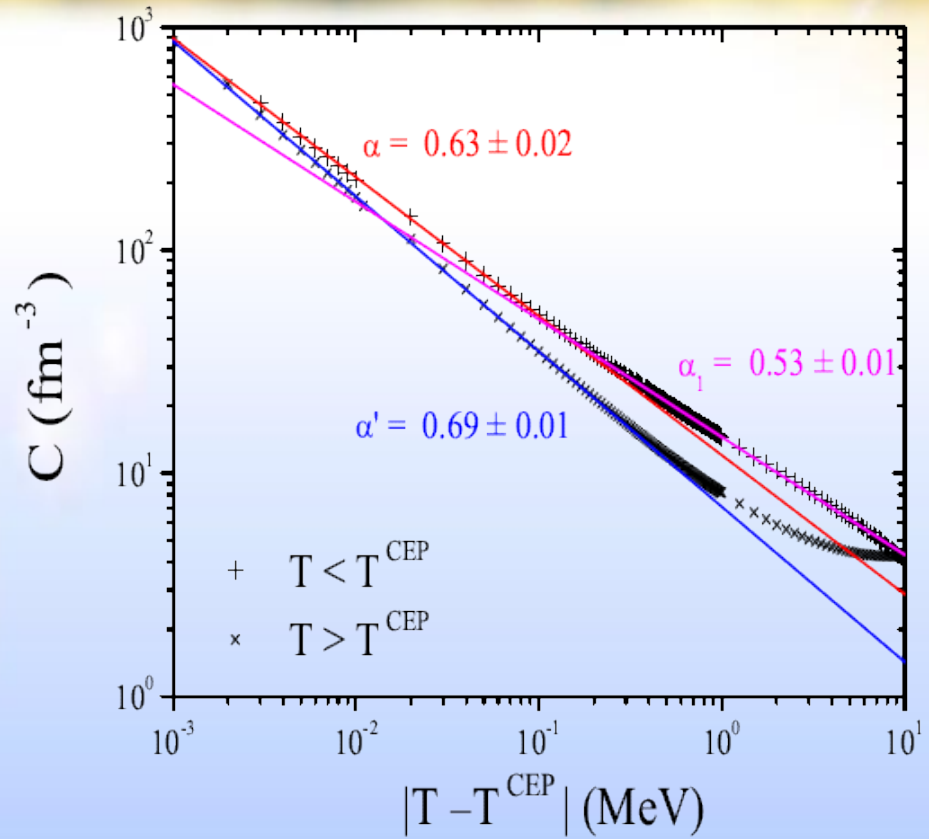
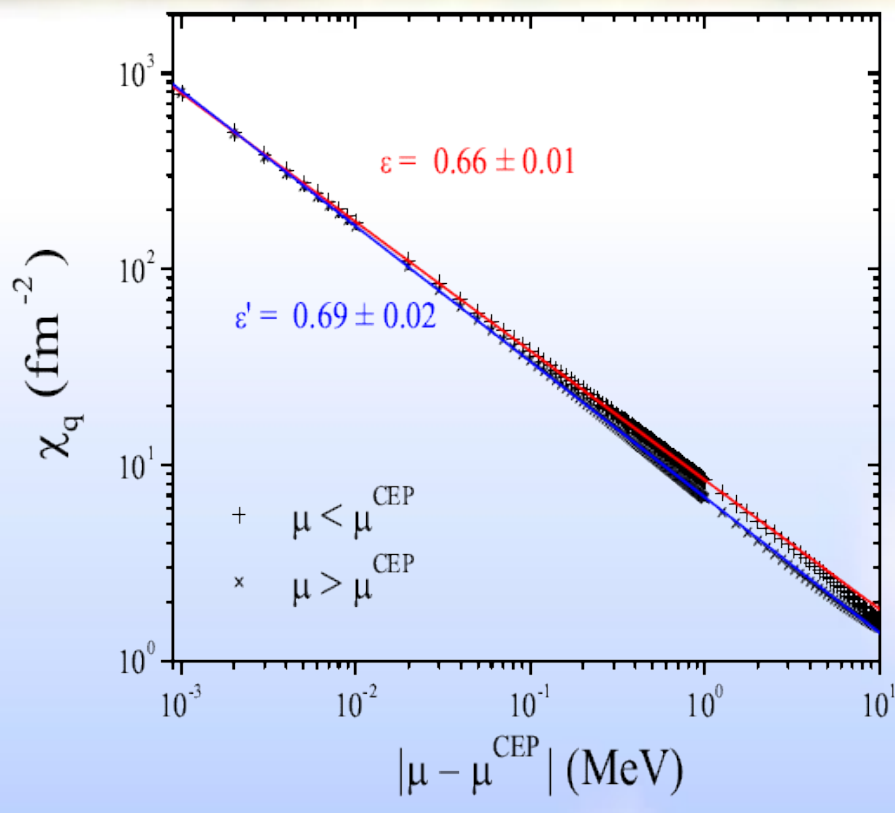
Fluctuations around the CEP



Left panel: Baryon number susceptibility as function of μ for different T around the CEP in PNJL model: $T^{CEP} = 169.11$ MeV and $T = T^{CEP} \pm 10$ MeV. Right panel: specific heat as a function of T for different values of μ around the CEP: $\mu^{CEP} = 321.32$ MeV and $\mu = \mu^{CEP} \pm 10$ MeV.

These behaviors of χ_q and C are qualitatively similar to those obtained in the SU(2) NJL model (Costa et al, PLB 647(2007) 431).

Critical behavior



Left panel: Baryon number susceptibility as a function of $|\mu - \mu^{CEP}|$ at the fixed $T = T^{CEP}$. Right panel: Specific heat as a function of $|T - T^{CEP}|$ at the fixed $\mu = \mu^{CEP}$.

For $|T - T^{CEP}| < 0.3$ MeV (respectively $|T - T^{CEP}| > 0.3$ MeV) the critical exponents are $\alpha = 0.63 \pm 0.02$ ($\alpha = 0.59 \pm 0.01$) and $\alpha_1 = 0.53 \pm 0.01$ ($\alpha_1 = 0.45 \pm 0.01$) \Rightarrow crossover of different universality classes, with the CEP being affected by the TCP.

Critical exponents

Quantity	C.E./path	PNJL	NJL	Universality
χ_q	$\varepsilon / \rightarrow \bullet$	0.66 ± 0.01	0.66 ± 0.01	$2/3$
	$\varepsilon' / \bullet \leftarrow$	0.69 ± 0.02	0.66 ± 0.01	$2/3$
	$\gamma_q / \rightarrow \bullet$	0.51 ± 0.01	0.51 ± 0.01	$1/2$
C	α / \bullet	$\alpha = 0.63 \pm 0.02$	0.59 ± 0.01	$2/3$
	α / \uparrow	$\alpha_1 = 0.53 \pm 0.01$	0.45 ± 0.01	—
	α' / \downarrow	0.69 ± 0.01	0.69 ± 0.01	$2/3$
	α / \bullet	0.50 ± 0.01	0.40 ± 0.02	$1/2$

Critical exponents (C.E.): the arrow $\rightarrow \bullet \left(\begin{array}{c} \bullet \\ \uparrow \end{array} \right)$ indicates the path in the μ (T) – direction to the CEP (TCP) for $\mu < \mu^{CEP}$ ($T < T^{TCP}$).

Model parameter effects

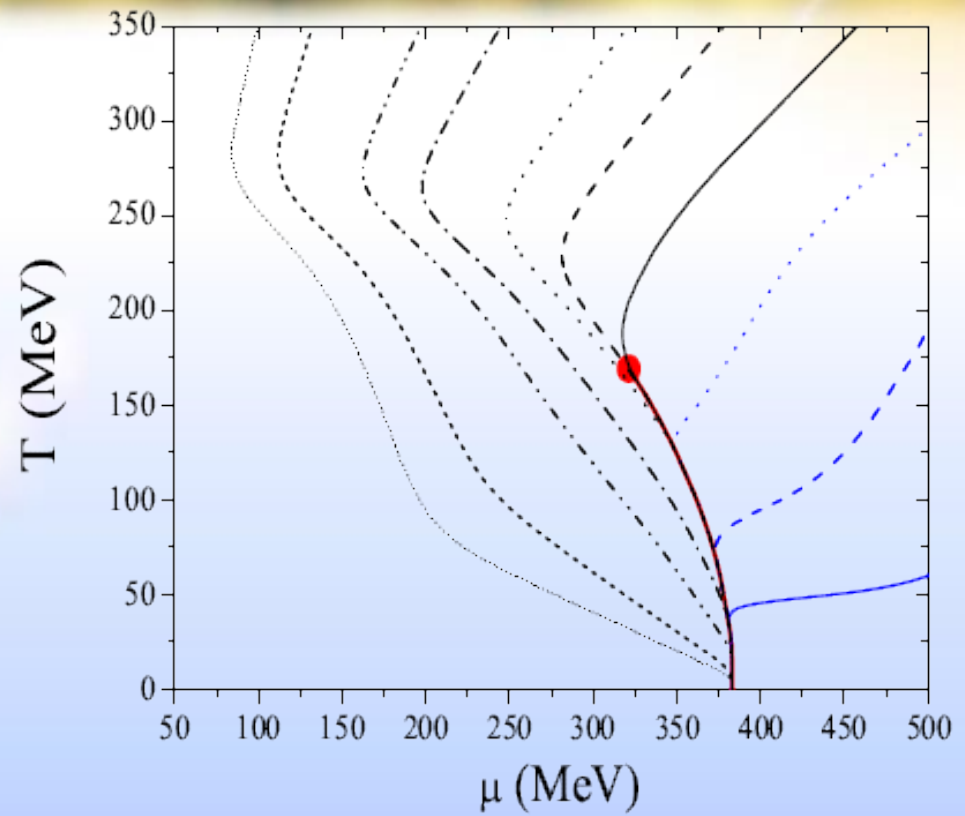
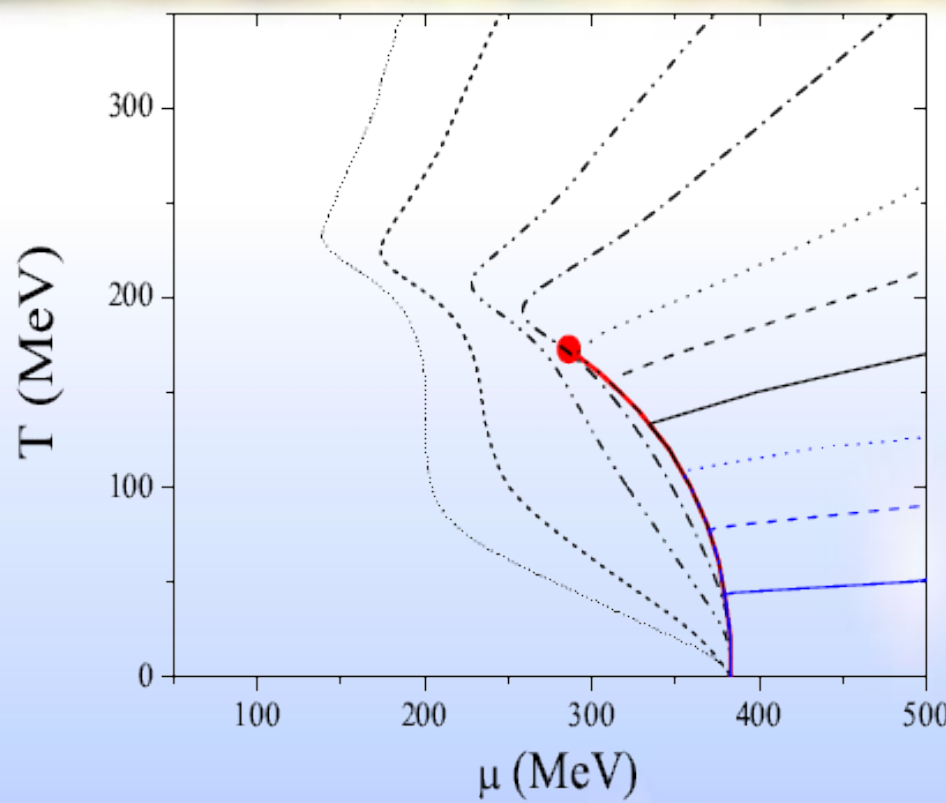
	Λ [GeV]	g [GeV $^{-2}$]	m [MeV]	$ \langle \bar{\psi}_u \psi_u \rangle ^{1/3}$ [MeV]	f_π [MeV]	m_π [MeV]	M [MeV]
Set A	0.590	2.435	6.0	241.5	92.6	140.2	400
Set B	0.651	5.04	5.5	251	92.3	139.3	335

Table 1: Set of parameters (Λ , g , m) used in the pure NJL model and the physical quantities chosen to fix the parameters. The constituent quark mass obtained is also included.

Parameter set	Regularization procedure	T^{CEP} [MeV]	μ^{CEP} [MeV]	T^{TCP} [MeV] (chiral limit)	μ^{TCP} [MeV] (chiral limit)
Set A	<i>Case I: $\Lambda \rightarrow \infty$</i>	172.48	286.35	206.50	192.87
	<i>Case II: $\Lambda = cte$</i>	169.11	321.32	207.66	270.80
Set B	<i>Case I: $\Lambda \rightarrow \infty$</i>	87.99	328.84	162.39	253.06
	<i>Case II: $\Lambda = cte$</i>	87.71	329.51	163.06	268.05

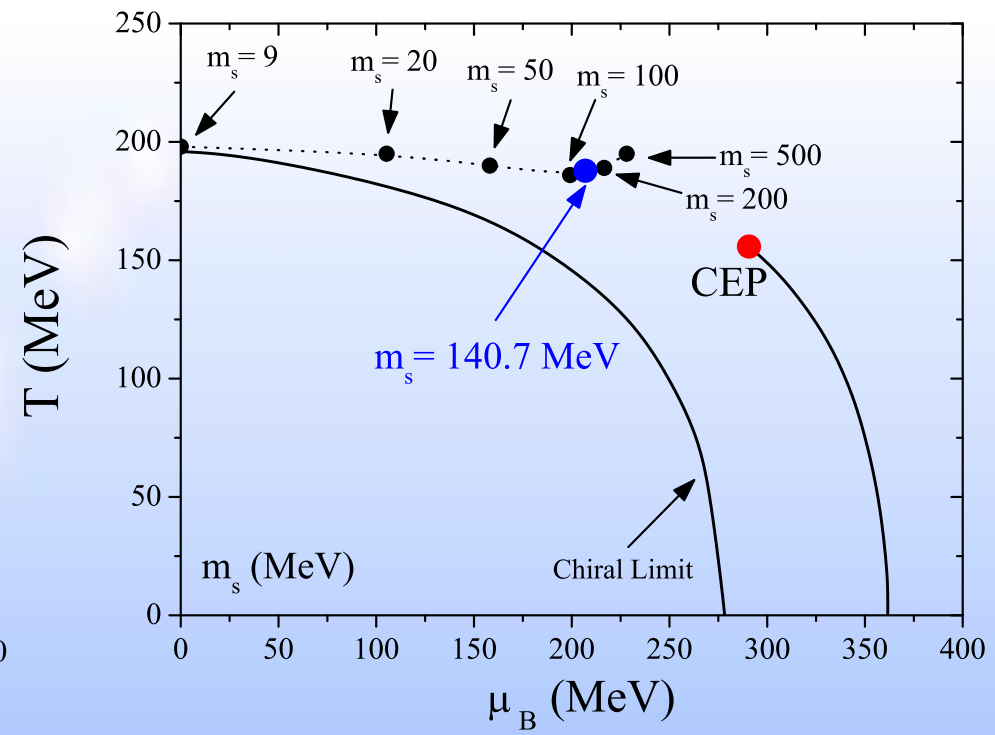
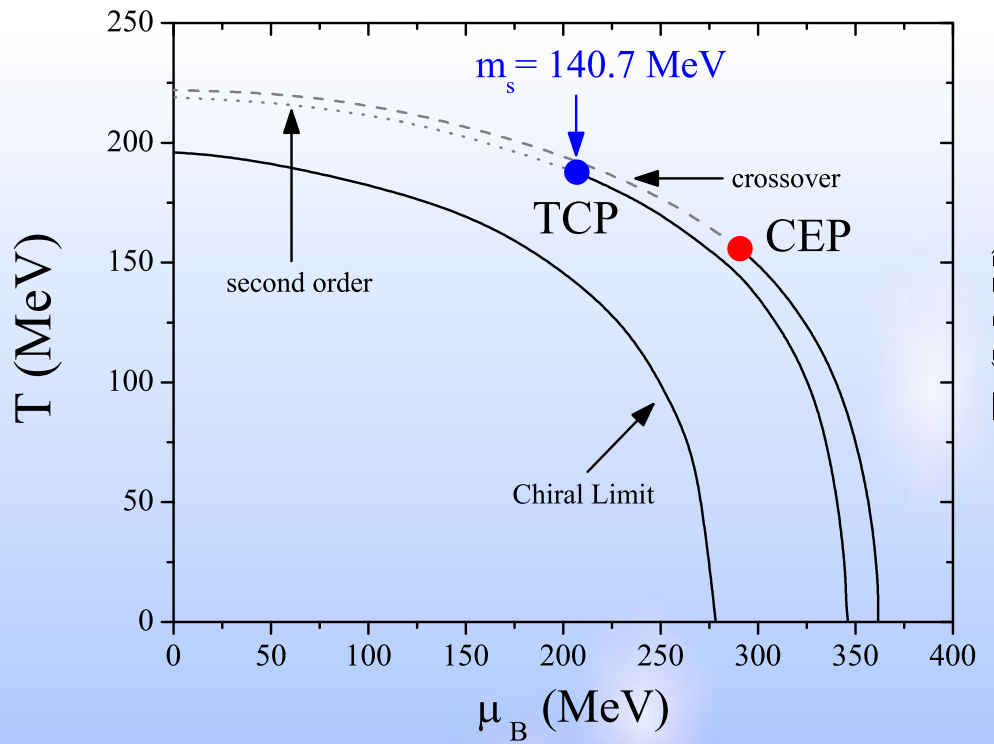
Table 2: Location of the CEP and the TCP at the (T, μ) plane for both sets of parameters and regularization procedures.

ISENTROPIC LINES AND THIRD LAW OF THERMODYNAMICS

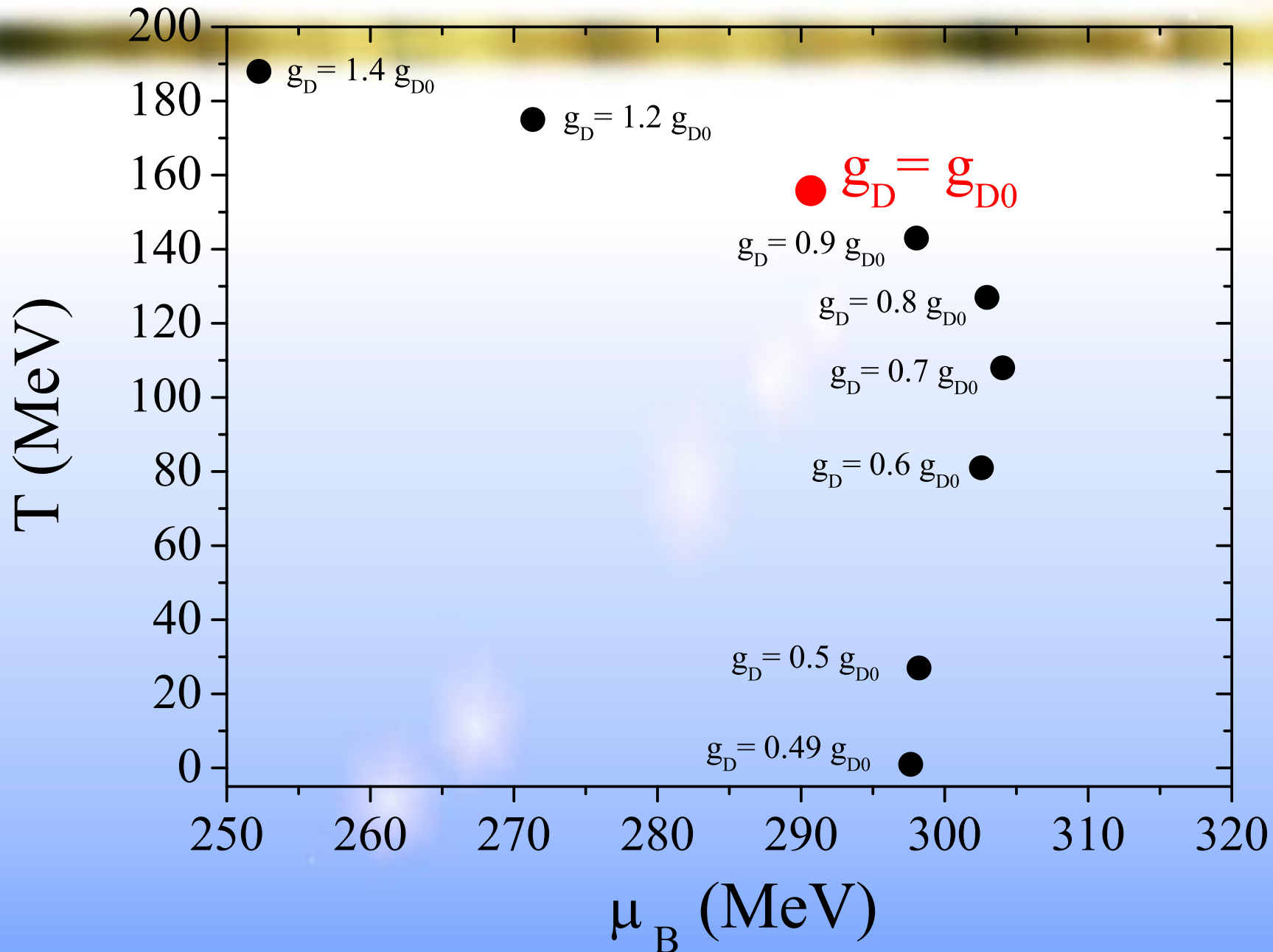


Isentropic trajectories in the $T - \mu$ plane for Case I (left panel) and Case II (right panel) using the parameter Set A. The following values of the entropy per baryon number have been considered: $s/\rho = 1, 2, 3, 4, 5, 6, 8, 10, 15, 20$ (from left to right).

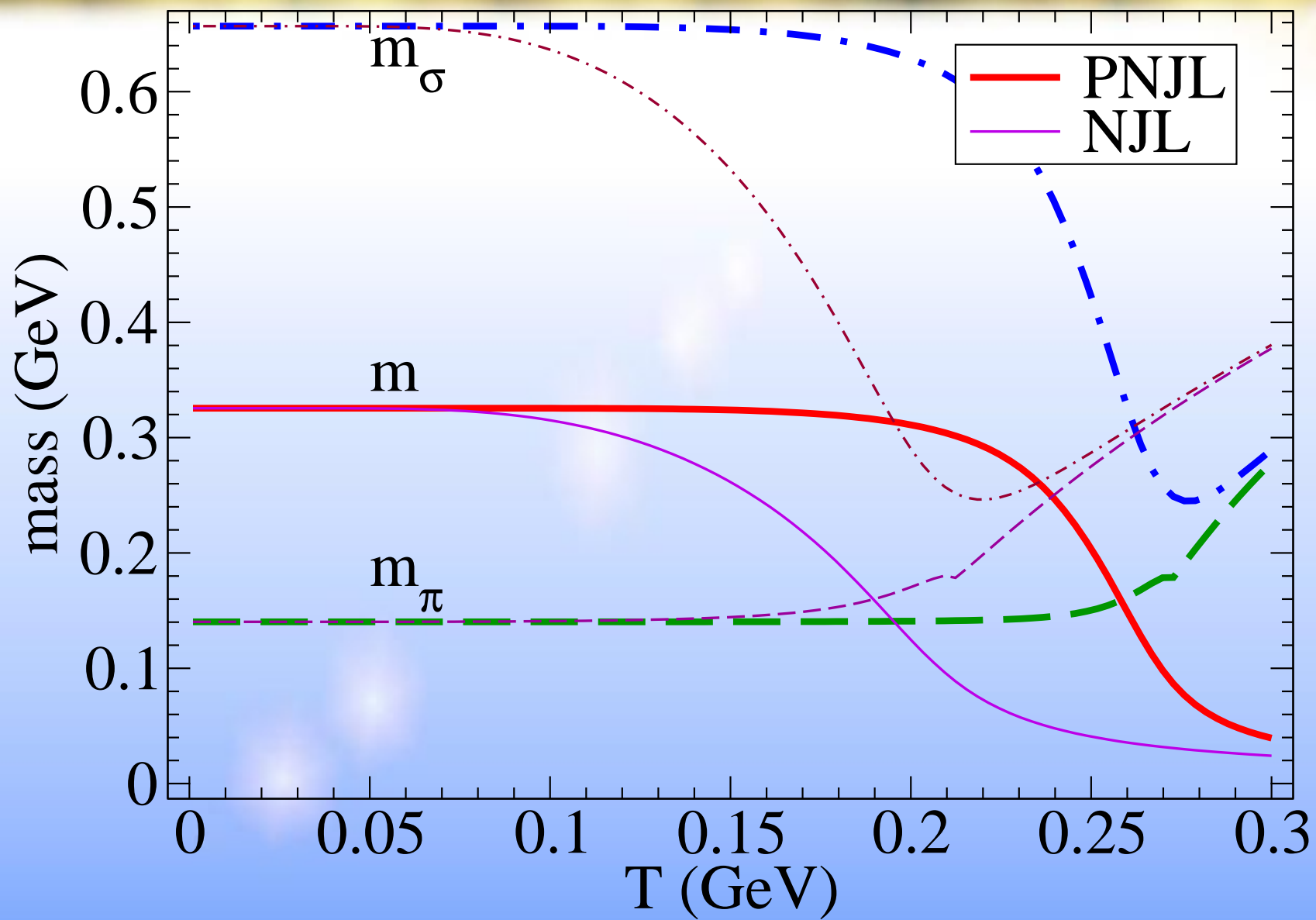
Phase diagram: evolution with the strange quark mass



Phase diagram: evolution with the t'Hooft interaction



Meson masses : NJL vs. PNJL at $\mu = 0$ GeV



Specificity of PNJL vs. NJL

Owing to the previous result, it is not possible to compare directly PNJL and NJL. We rescaled the temperature to study NJL vs PNJL in three sectors: below T_c , around T_c and above T_c .

✿ Two definitions for the chiral T_c

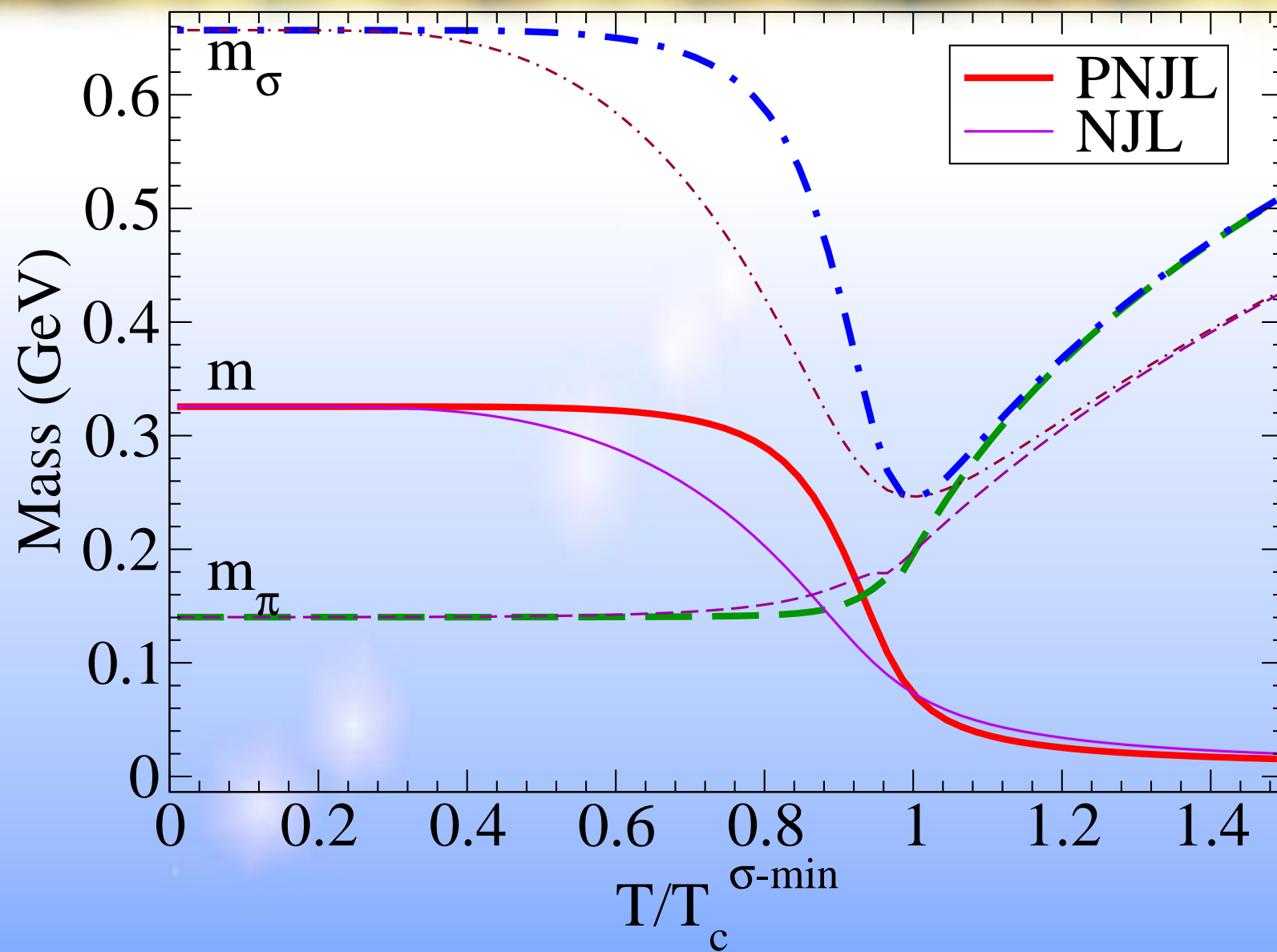
At the chiral limit, the restauration of the chiral symmetry characterizes itself by $m(T \rightarrow T_c) \rightarrow 0$ AND $m_\pi = m_\sigma$ (strictly speaking, $F_\pi(\omega) = F_\sigma(\omega)$).

When we add an explicit symmetry breaking, ($m_0 \neq 0$), none of these phenomena occur.

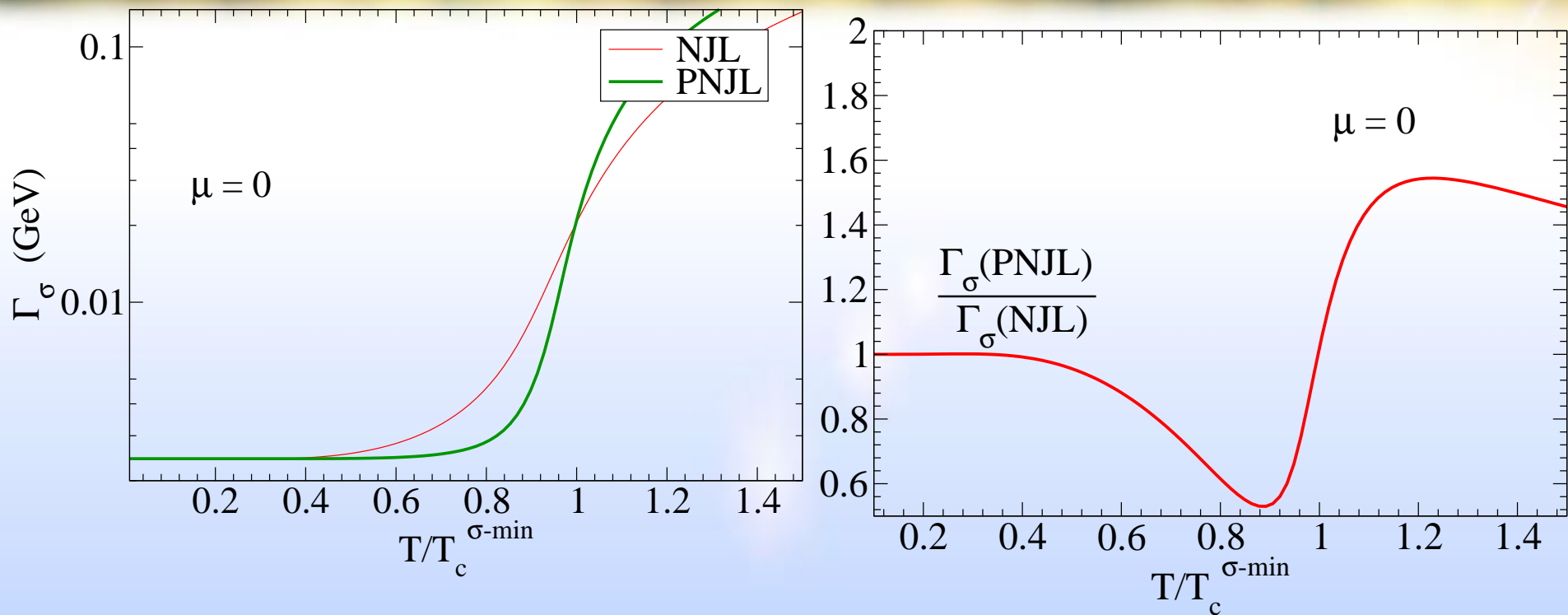
One defines $T_c^{\chi-\text{crossover}}$ as the maximum of $\frac{-dm}{dT}$ and $T_c^{\sigma-\min}$ as the minimum of $m_\sigma(T)$.

We will use $T_c^{\sigma-\min}$ as our rescaling temperature (temperature characteristic of the restauration of the chiral symmetry *i.e.* $f_\pi \rightarrow 0$).

Meson masses : NJL vs. PNJL at $\mu = 0$ GeV



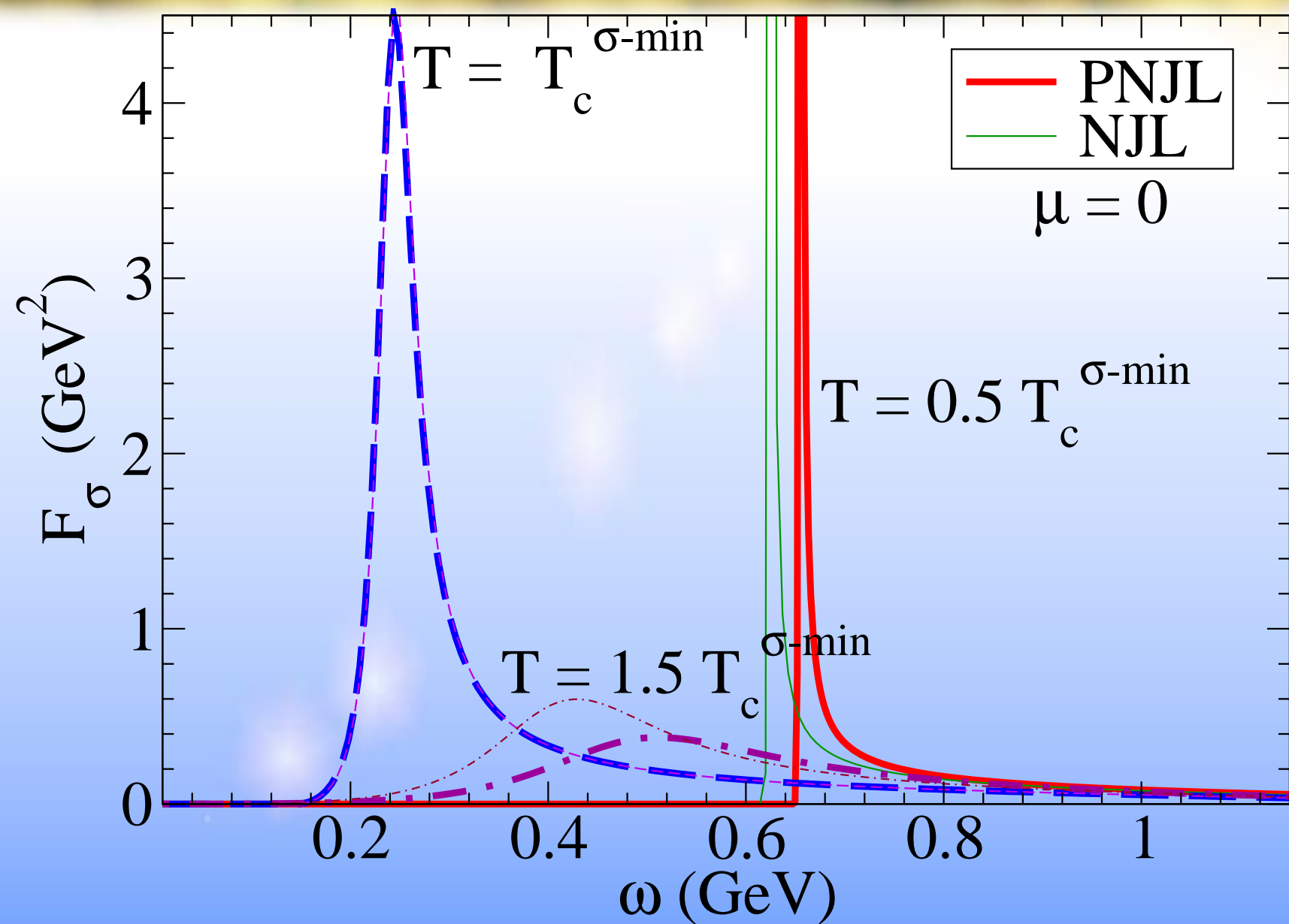
Comparison NJL vs. PNJL: width of the σ



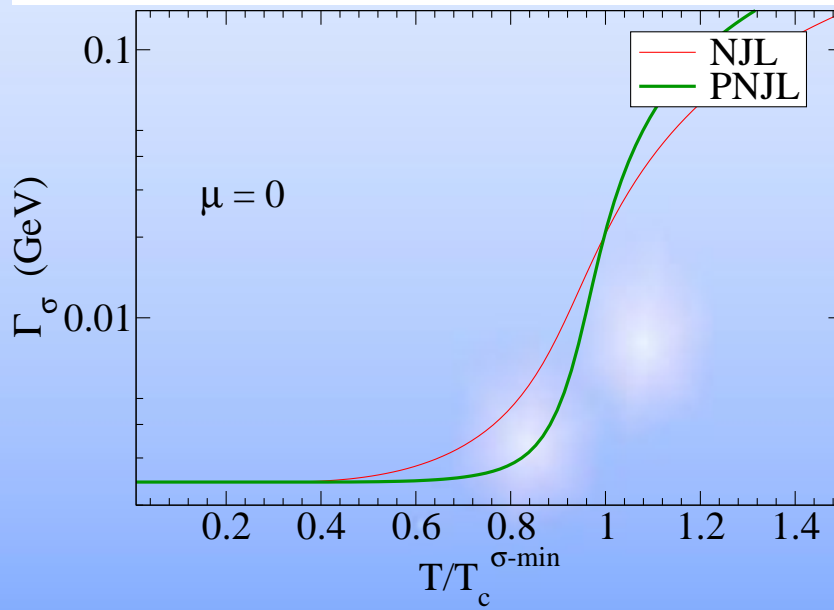
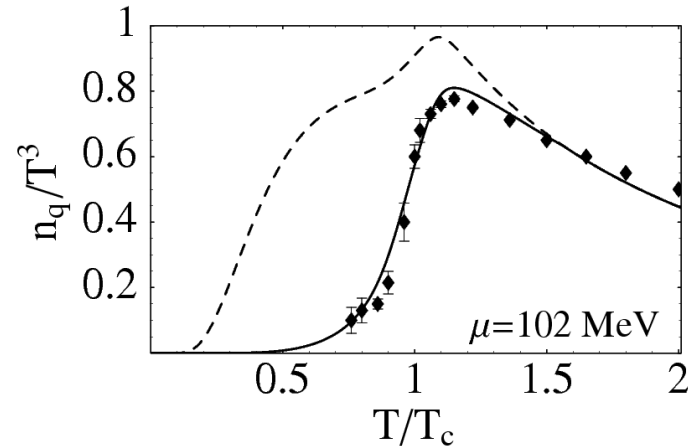
Evidence of a quantitative effect toward confinement ; Criterion $T_c^{\sigma\text{-min}}$ OK.

Mesonic correlation functions at finite temperature and density in the Nambu-Jona-Lasinio model with a Polyakov loop. H. Hansen, W.M. Alberico, A. Beraudo, A. Molinari, M. Nardi, C. Ratti, Phys. Rev. D75:065004, 2007.

Comparison between σ spectral function in NJL and PNJL



As an intermediate conclusion : Two evidences of confinement ?



Quantitative improvement of both results toward confinement, at mean field order (n_q) and at RPA order (width)

No confinement mechanism: there is no dynamical gluonic degrees of freedom or other features which would explain qualitatively the description of the quark confinement.